International Journal of Disaster Risk Reduction 93 (2023) 103771

Contents lists available at ScienceDirect

International Journal of Disaster Risk Reduction

journal homepage: www.elsevier.com/locate/ijdrr

Quantifying the effects of nature-based solutions in reducing risks from hydrometeorological hazards: Examples from Europe

Mohammad Aminur Rahman Shah [a, b], Jiren Xu [c, b], Francesca Carisi [d], Francesco De Paola [e], Silvana Di Sabatino [f], Alessio Domeneghetti [g], Carlo Gerundo [e], Alejandro Gonzalez-Ollauri [h], Farrokh Nadim [i], Natasha Petruccelli [g], Annemarie Polderman [j], Francesco Pugliese [e], Beatrice Pulvirenti [k], Paolo Ruggieri [f], Giuseppe Speranza [e], Elena Toth [g], Thomas Zieher [j], Fabrice G. Renaud [b, *]

[a] Canadian Centre for Climate Change and Adaptation, University of Prince Edward Island, Charlottetown, PEI, Canada
[b] School of Interdisciplinary Studies, University of Glasgow, Dumfries, UK
[c] Water@leeds, School of Geography, University of Leeds, Leeds, UK
[d] Interregional Agency for the Po River (AIPO), Parma, Italy
[e] Department of Civil, Architectural and Environmental Engineering (DICEA), University of Naples Federico II, Naples, Italy
[f] Department of Physics and Astronomy, University of Bologna, Bologna, Italy
[g] Department of Civil Chemical Environmental and Materials Engineering (DICAM), University of Bologna, Bologna, Italy
[h] BEAM Research Centre, School of Computing, Engineering, And Built Environment, Glasgow Caledonian University, Glasgow, UK
[i] Norwegian Geotechnical Institute, Oslo, Norway
[j] Institute for Interdisciplinary Mountain Research, Austrian Academy of Sciences, Innsbruck, Austria
[k] Department of Industrial Engineering, University of Bologna, Bologna, Italy

ARTICLE INFO

Keywords:
Hydrometeorological hazards
Nature-based solutions
Risk assessment
Social-ecological systems
Scenarios
OPERANDUM
PHUSICOS

ABSTRACT

The combination of climate change and social and ecological factors will increase risks societies face from hydrometeorological hazards (HMH). Reducing these risks is typically achieved through the deployment of engineered (or grey) infrastructure but increasingly, nature-based solutions (NBS) are being considered. Most risk assessment frameworks do not allow capturing well the role NBS can play in addressing all components of risk, i.e., the hazard characteristics and the exposure and vulnerability of social-ecological systems. Recently, the Vulnerability and Risk assessment framework developed to allow the assessment of risks in the context of NBS implementation (VR-NBS framework) was proposed. Here, we carry out the first implementation of this framework using five case study areas in Europe which are exposed to various HMH. Our results show that we can demonstrate the effect NBS have in terms of risk reduction and that this can be achieved by using a flexible library of indicators that allows to capture the specificities of each case study hazard, social and ecological circumstances. The approach appears to be more effective for larger case study areas, but further testing is required in a broader variety of contexts.

1. Introduction

Globally, disasters from hydro-meteorological hazards (HMH) such as floods, droughts and landslides are increasing [1]. Risks related to some of these hazards will be exacerbated by the consequences of climate change [2] and other factors linked to socio-

* Corresponding author.
E-mail address: Fabrice.Renaud@glasgow.ac.uk (F.G. Renaud).

https://doi.org/10.1016/j.ijdrr.2023.103771
Received 30 January 2023; Received in revised form 24 May 2023; Accepted 25 May 2023
Available online 25 May 2023

economic development and policies, such as the increased vulnerability of population and ecosystems and increased exposure linked to population growth and settlement in hazard-prone areas. Reducing risks to HMH and other hazards is, therefore, a priority to limit their negative impacts on populations and infrastructure and to preserve development gains globally [3].

To reduce exposure to HMH, engineered structures (or grey infrastructure) such as sea walls, dykes, levees and retaining walls are generally used. However, there is an increasing interest in and uptake of green infrastructure such as nature-based solutions (NBS) as an alternative or complement to grey infrastructure. Nature-based solutions are defined as "actions to protect, conserve, restore, sustainably use and manage natural or modified terrestrial, freshwater, coastal and marine ecosystems, which address social, economic, and environmental challenges effectively and adaptively, while simultaneously providing human well-being, ecosystem services and resilience and biodiversity benefits" [4]. Disaster risk reduction (DRR) and climate change adaptation and mitigation are two of the societal challenges considered by IUCN to potentially be addressed by NBS [5].

Many assessment frameworks for evaluating the effectiveness of grey and/or green infrastructure (including NBS) have been developed in recent years. Most of these frameworks are indicator-based approaches to characterise and quantify risks to natural hazards (e.g., Refs. [6–8]). Many frameworks now consider integrated social-ecological systems (SES) as the unit of analysis, but there remains a preponderance of social indicators being used to quantify risks (e.g., Refs. [9–12]). This poses a problem in characterising the vulnerability and exposure of SES adequately. It also does not allow capturing the fact that NBS can contribute to reducing risks on all its dimensions, namely the hazard characteristics (e.g., by allowing increased infiltration, therefore, helping to reduce in some cases the frequency and magnitude of floods and droughts), the vulnerability (e.g., by enhancing livelihoods through the provision of ecosystem services) and the exposure (e.g., by serving as a physical buffer between hazard location and settlements/infrastructure) [11]. This is linked to the fact that NBS can provide multiple benefits, which is not often the case with grey infrastructure [13,14]. Efforts have recently been made to better capture the role ecosystem-based approaches can play in reducing risks through developing new frameworks [9,11,12,15,16] and indicator libraries [7,11,12,17].

Recently, Ref. [11] have proposed a conceptual framework for vulnerability and risk assessment of SES in the contexts of NBS (VR-NBS framework; Fig. 1). This paper aims to present the first series of risk assessments carried out with the VR-NBS framework and quantify the effects of NBS in reducing risks from hydrometeorological hazards. This is done to test the feasibility of the framework and to determine if experts who have not been involved in the development of the framework can use it with no major difficulties. The research was carried out in the context of the OPERANDUM project (OPEn-air laboRAtories for Nature baseD solUtions to Manage hydro-meteorological risks, https://www.operandum-project.eu/oals/), which aimed to reduce risks from HMH through the co-development and co-deployment of NBS in various European countries. The research in the project was based on so-called Open Air Laboratories (OAL) where the NBS were initiated and implemented with different stakeholders. OALs are pilot research infrastructures that generalise and specialize the living laboratory concept to the co-design and co-development of NBS (see https://geoikp.operandum-project.eu/oal/explorer). The VR-NBS framework was also applied for risk assessment into two Demonstrator Cases (DC) of the PHUSICOS project (https://phusicos.eu/), a sister project of OPERANDUM, whose experts were not involved in the development of the framework. The DCs are the demonstration sites where NBS projects are being implemented under the PHUSICOS project. We have selected these OALs and DCs as these sites present different hazards and NBS contexts, and sufficient data related to risk assessment and NBS project design and implementation is available. This helps to present suitable cases for demonstrating the application of the VR-NBS framework for quantifying the effects of NBS for reducing risk. We present here risk assessments and deter-

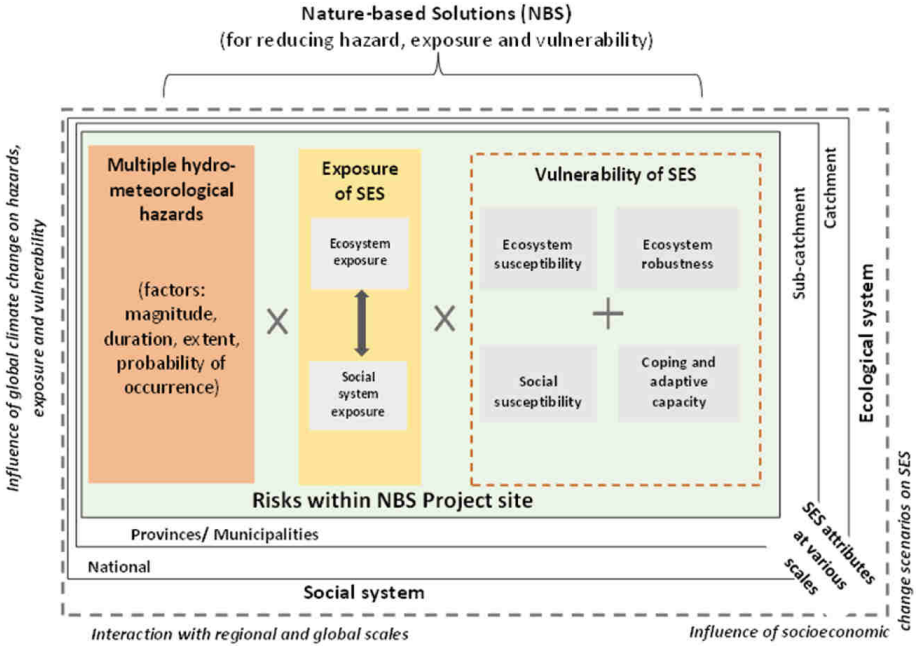

Fig. 1. Conceptual framework for vulnerability and risk assessment of SES in NBS project sites (VR-NBS) (adapted from Ref. [11].

mine the effect of NBS for reducing risk from landslides (OAL Austria and OAL United Kingdom), rockfall (French DC) and floods (OAL Italy, Norwegian DC) and discuss the functionalities of the VR-NBS, both in terms of advantages and limitations.

2. The VR-NBS framework

We used the VR-NBS framework as a basis to quantify disaster risk using an index-based approach for our five case studies. This framework, originally developed using the main concepts of the Delta-SES framework [9], computes risk as Hazard × Exposure × Vulnerability [18,19] (Fig. 1). NBS projects are usually designed to reduce risks by three possible ways: modifying hazard characteristics, reducing exposure of SES to hazards, and reducing the vulnerability of the SES (Fig. 1). The VR-NBS framework proposes specific indicators for hazards, exposure and vulnerability in a flexible indicator library [11].

The VR-NBS framework considers the geographical boundary of NBS projects, usually a smaller area (part of a river floodplain, lake, slope of a hill or segment of a coast), and the components of the social system (including all social, economic, governance/institutional aspects) and ecosystem features (including all environmental/ecological components) within that area as the basic space for risk assessment. Some social and ecological elements, such as policies and climatic/hydrological characteristics, are linked to larger spatial scales, which are also considered in the risk assessment and can be characterized by specific indicators. The framework also considers single or multi-hazard contexts that could be experienced at the NBS project sites. Indicators related to hazard characteristics, such as magnitude, duration, extent and probability of occurrence, are used for calculating the hazard index. The exposure component of the framework includes the social and ecological elements within NBS project sites exposed to hazards. The vulnerability component of the framework consists of four vulnerability domains: social susceptibility, ecosystem susceptibility, ecosystem robustness, and coping and adaptation capacities of the social system (as per [9]). Separate indicators for each vulnerability component are used in the first instance and then aggregated to assess the overall vulnerability of the SES.

The framework can be used to compute risk at different time intervals of an NBS project. In many cases, NBS will only reach the maximum risk reduction capacities they are designed for months or years after their implementation, i.e., the time it takes for the NBS matures. Therefore, the indicator framework needs to allow capturing this temporal dimension to determine when the maximum risk reduction capacity is reached and to allow the implementation of additional measures until this risk reduction capacity is reached. Indicators for risk assessment should be prioritised and used in repeat assessments during the maturation phase of the NBS. The results of this analysis could, for example, prompt the integration of engineered structures alongside the NBS if NBS maturation, and therefore its capacity to reduce risks, takes a long time. Since many NBS projects rely on the growth of organic elements (e.g., plants), which are also influenced by seasonal climatic variability, indicators that can capture the effect of seasonality should also be considered. The framework suggests that, for greater understanding, risk must be assessed multiple times during different seasons throughout the NBS project maturation stages. Continuous monitoring should be conducted to ensure that the risk reduction benefits of the NBS projects are delivered in the long run.

Along with the conceptual VR-NBS framework, Ref. [11] also provided an indicator library containing 135 indicators covering exposure and vulnerability components of risk assessment. In this study, we have used this indicator library as a primary source for identifying suitable indicators for risk assessment at our case study sites. The selected indicators and data collection methods, and detailed risk calculation process are described in the following sections.

3. Materials and methods

3.1. Study areas and implemented nature-based solutions

This study considers five sites across Europe where NBS projects are implemented/planned under the OPERANDUM and PHUSICOS projects. A summary of the case study sites is presented in Table 1 and detailed information for each site is presented in the following sections.

3.1.1. OAL Italy - Panaro River

OAL Italy is located in the Emilia-Romagna region, and it includes three sites where NBS are implemented and tested. In one site on the coast (Volano/Bellocchio), NBS to mitigate coastal erosion and storm surge are tested. Another site is on the delta of the river

Table 1
OALs and DCs considered in this study.

OALs and DCs	Area and spatial coverage	Natural hazard	NBS implemented/planned
OAL Italy (Panaro river basin, Emilia-Romagna region, Italy)	1775 km^2, covers 22 municipalities	Flooding	Installing herbaceous plants on the embankment of the Panaro River to reduce soil erosion and strengthen the embankment
OAL Austria (Watten valley, Tyrol, Austria)	0.25 km^2, within one municipality	Landslide	First NBS: sealing off leaky streams and channels in the upslope contributing area Second NBS: optimization of the forest management
OAL UK (Catterline Bay, Aberdeenshire, Scotland)	0.23 km^2, within one municipality	Landslide	NBS include soil and water bioengineering techniques such as live pole drains, live cribwalls, brush layers, live slope lattice, live palisades, high-density planting of native woody species
Norwegian DC (Øyer, Gudbransdalen Valley, Norway)	0.43 km^2, within one municipality	Flooding	NBS project includes the creation of a creek bed instead of a 600 mm diameters pipeline
French DC (Artouste, Pyrenees, France)	0.31 km^2, within one municipality	Rockfalls	The NBS project consists of wooden tripods and wooden meshes made of larch trunks, fixed to the ground or anchored in the bedrock at different depths.

Po (Po di Goro) and deals with salt-wedge intrusion. Finally, an inland site, the Panaro river (hereafter OAL Italy Panaro) is where an NBS to reduce risks from river flooding is implemented. The latter is one of the study areas used in this work. The river Panaro is a tributary of the Po River and flows for its greatest part in the province of Modena (Northern Italy), with a basin covering a surface of 1775 km^2, 45% of which is in the mountain environment (Fig. 2). The Panaro basin covers 22 municipalities and is the largest and most populated area of all OAL sites considered by the OPERANDUM project, with many industrial and agricultural activities (land-use shown in Fig. 2). The basin is exposed to riverine flooding, experiencing inundations in recent decades as a consequence of isolated storms or mesoscale organised convection. Such events bring the risk of loss of human life, damage to properties and infrastructures, damage to agriculture and livestock, and disruption of both tourism activities and economic activities [20]. The NBS aims to mitigate these risks by installing herbaceous plants on the embankment of the Panaro River (https://geoikp.operandum-project.eu/oal/explorer/italy-panaro-river), with the intent to reduce soil erosion on the internal toe of the riverbank, as well as potentially contribute to preventing uncontrolled superficial erosion of the levee in case of overtopping).

3.1.2. *OAL Austria - Vögelsberg landslide, Watten Valley, Tyrol*

OAL Austria – the Vögelsberg landslide – is located in the lower Watten valley, Tyrol, Austria - south of the town of Wattens. The OAL includes the hydrological catchment of about five square kilometers ranging from 750 to 2200 *m* a.s.l, and the active landslide of about 0.25 km^2 area situated at the lower end of the slope (Fig. 2). The activity of the landslide is mainly controlled by groundwater recharge and accelerates after 'wetter than normal periods' including snowmelt seasons [22,23]. The landslide's activity can lead to cascade effects, including debris flows and shallow landslides at the foot slope [24]. The currently active (landslide movement) area is covered by agricultural areas, including meadows and pasture and local forest patches (land use shown in Fig. 2). Nine houses and

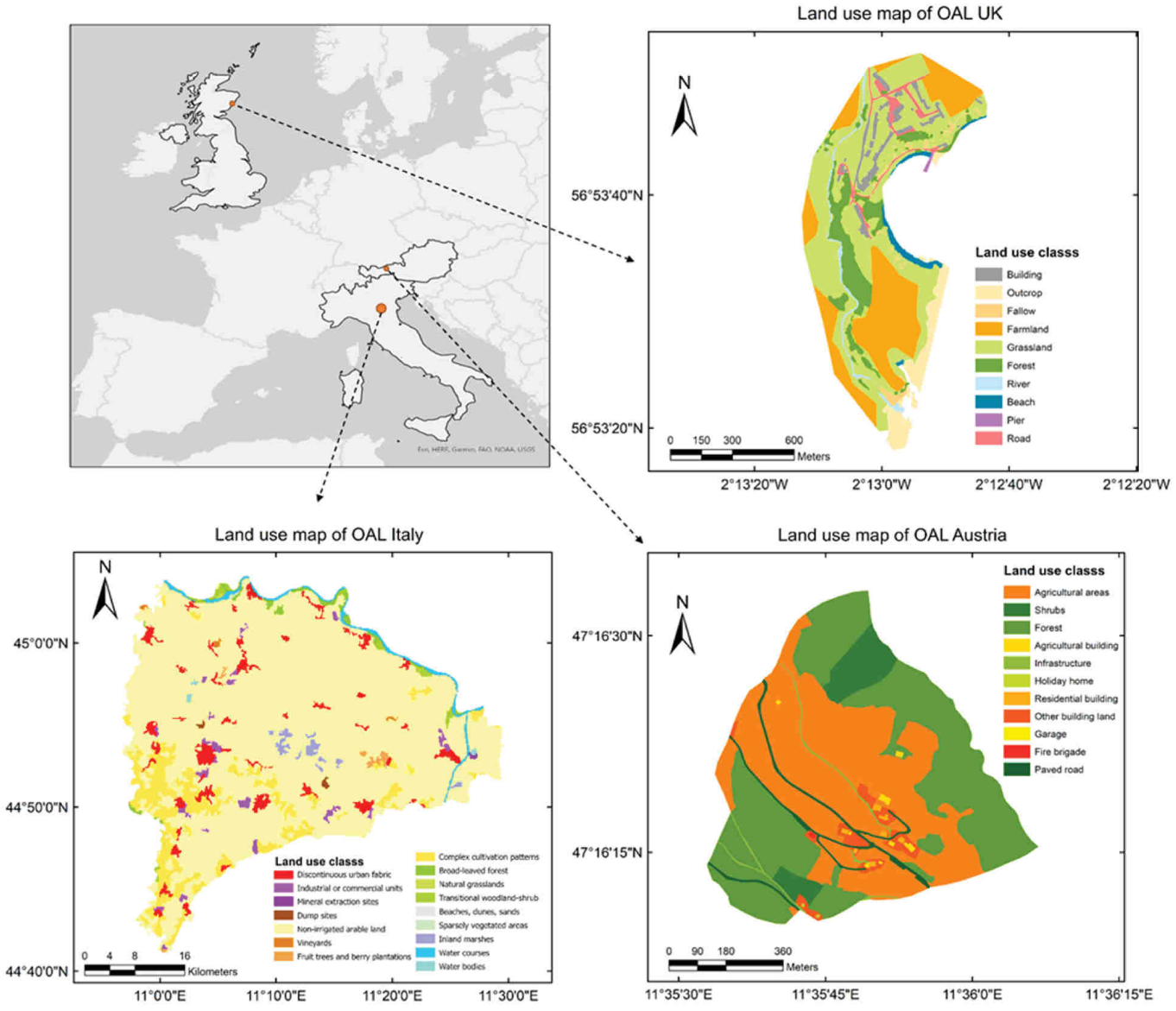

Fig. 2. Land use maps of OAL Italy Panaro, Austria, and the UK which were derived from the Corine Land Cover 2018 dataset [21] and project maps from OALs.

several farm buildings and infrastructure (e.g., roads, power lines and water supply pipeline) are present in the active area, showing signs of damage due to the ground motion.

The first NBS consists in sealing off leaky streams and channels in the upslope contributing area, which helps to reduce the activity of the deep-seated landslide by tackling the infiltrating water and the related increase of the pore water pressure. The first NBS tested in OAL Austria includes a prototype of a fully bio-degradable bentonite mat, which is a composite of geotextile layers enclosing a layer of clay material (bentonite) with high swelling potential under saturation. The supporting geotextile layers degrade over time, but the impermeable clay layer persists and guarantees the desired effects over a long time spans (https://www.operandum-project.eu/oal/austria/). The second NBS is the optimization of forest management, which is currently in the modelling stage. The forest upslope of the landslide in OAL Austria is mainly composed of Norway spruce (*Picea abies*) in varying density and age. Optimizing the forest management by introducing mixed forests that facilitate multiple vegetation layers will reduce the amount of groundwater recharge by a more effective rainfall interception and higher transpiration. Under current crown coverage conditions in the very densely stocked commercial spruce forests, no low vegetation is present (*Piceetum nudum*) in most parts of the forest due to the unfavorable light conditions. Reducing the crown coverage of these forests to 70–90% will help introducing low vegetation layers, enhancing the hydrological effects of the mountain forest and reducing the main driver of the deep-seated landslide.

3.1.3. OAL UK - Catterline Bay, Aberdeenshire, Scotland

OAL UK covers an area of 0.23 km^2 and is located adjacent to Catterline Bay, approximately 10 km south of the village of Stonehaven, Aberdeenshire, on the Northeast coast of Scotland (Fig. 2). The OAL has an outstanding natural beauty, made famous by the Scottish painter Joan Eardley. The site is subject to shallow landslides triggered by surface water accumulation following prolonged, heavy rainfall events and outflow from natural springs, as well as coastal and surface erosion due to the site's sloped topography and its proximity to the sea (land use shown in Fig. 2).

The soil along the OAL's slopes and cliffs is a cohesive mixture of silty sand with relatively high clay content (e.g., Refs. [25,26]). The site has a shallow bedrock of conglomerates and it has changing cohesive properties when subjected to changing wetting and drying cycles, making it prone to landslides and erosion following heavy rainfall. The community of Catterline and their houses are atop the sea cliffs; thus, landslides and coastal erosion pose a direct risk to lives and properties. The community has less than 200 residents with a lower rate of unemployment, higher income, better housing and health outcomes when compared to the national average [8].

The NBS implemented in OAL UK include soil and water bioengineering techniques such as live pole drains (i.e., a drainage system constructed using natural, sustainable materials), live cribwalls (i.e., an engineered retaining wall built with locally available natural, organic materials), brush layers (i.e., slope terraces reinforced with live fascines and cuttings), live slope lattice (i.e., a slope skin built from a lattice of timber logs supplemented with live cuttings), live palisades (i.e., a wooden barrier built with timber stakes and logs and then backfilled with earth, organic and living plant materials), high-density planting of native woody species such as willow and maple, and live ground anchors (i.e., platipus ground anchors supplemented with biodegradable geogrid mats and plant seeds; details of these NBS are available in https://www.operandum-project.eu/scotland-uk/). In the present study, we used high-density planting of willow and maple as the NBS example because spatially-distributed modelling data were available for analysis under current and future climate change scenarios.

3.1.4. Norwegian DC – Øyer, Gudbransdalen Valley

Gudbrandsdalen Valley is one of the Demonstrator Cases (DCs) of the PHUSICOS project. It is one of the most populated rural areas in Norway, extending for roughly 140 km from the town of Lillehammer, on the south side, to the village of Dombås, in the north. The wide floodplains extending along the river, which are mostly farmland dotted with many scattered residential settlements, are exposed to a range of hydro-meteorological hazards, flooding by the main river and by the tributary rivers, debris flows and debris slides, rockfall and snow avalanches. One of the case studies of this DC is located in Trodalen, a small residential area (approximately 50 inhabitants) belonging to the Municipality of Øyer in Innlandet County, located nearby Ramfjord forest and in between the river Søre Brynsåa and the creek Todalsbekken. The former use of the area was gravel outtake and is partly occupied by an abandoned gravel pit that the municipality plans to develop into a new housing area (200 new residential units with an expected population of 500). Further development of the area has been put on hold due to a lack of flood protection (land use shown in Fig. 3).

The core of the NBS design project is the creation of a creek bed instead of a 600 mm diameter pipeline to increase its conveyance capacity during a flood situation. The pipeline is 120 *m* long, crossing under a road, and has its outlet in the Søre Brynsåa river. This work is currently under implementation, and it is going to be coupled with a buffer zone in the lower part of the housing development which will have a double aim: serving as a retention measure during floods and as a blue-green nature park for inhabitants for the rest of the time.

Since open watercourses are more robust and therefore prone to deal with floods, the NBS proposed by PHUSICOS is expected to increase safety for residents and users of the area, including children, to achieve money saving in the event of floods, as it is more costly to repair than to prevent damages, and to produce a positive impact on the biodiversity in the area due to the creation of new habitat for species associated with water (details of these NBS are available in https://phusicos.eu/case_study/valley-of-gudbrandsdalen-norway/).

3.1.5. French DC– Artouste, Pyrenees

The Pyrenees DC is located in Artouste, within the Municipality of Laruns, in the Atlantic Pyrenees department, along a primary regional road (RD-934 – A-136) connecting several small towns located along the Spain-France borders. On RD-934 an average daily traffic intensity ranging between 1500 and 2500 vehicles/day moves with a peak of more than 3000 vehicles/day during summer and winter weekends. The DC is a forested slope located approximately at the progressive 46.8 km of the RD-934, in the foothill area of

Fig. 3. Land use maps of PHUSICOS Norwegian and French DCs which were derived from in-house maps from DCs.

mount Pic Lavigne (2018 *m* a.s.l.). Here the risk of rockfalls is relevant due to the presence of a steep rocky slope, with a slope angle > 40°, covered by a forest, where many rocky scarps and isolated blocks can trigger rockfall events which can show variable intensity, ranging from small blocks to boulders greater than 1 m^3. Specifically, a rocky front, about 200 *m* from the road, is significantly susceptible to collapse. The current forest cover is characterized by medium-low tree density and the tree average diameter is rather limited, thus not being able to provide enough protection against large rockfalls. The road segment exposed to the invasion of collapsed boulders is about 700 *m* long and is only partially protected by pre-existing and under-construction defence structures (rockfall tunnel and rockfall fences, respectively), along the main rockfall corridors (land use shown in Fig. 3).

The NBS designed and currently under implementation in the frame of the PHUSICOS project consist of wooden tripods (fixing individual boulders) and wooden meshes (fixing grouped boulders and fractured rock masses) made of larch trunks (15 cm diameter), fixed to the ground or anchored in the bedrock at different depths. These interventions are designed to fix and stabilize rock boulders with masses larger than 1500 kg. Along with these structures, masonry walls were designed to locally support some overhanging portions of rock faces. They are completed with 2.25 *m* tall and 3–5 *m* long wooden barriers, made of larch trunks (25 cm diameters), placed near the main release areas to stop boulders as soon as they collapse (details of these NBS are available at https://phusicos.eu/case_study/the-pyrenees-spain-france-andorra/).

3.2. VRA indicators and data collection

The exposure and vulnerability indicators (including potential proxy indicators) for each OAL were selected based on the indicator library provided by Ref. [11] as well as discussions with the OAL partners in the OPERANDUM project. Some of these indicators are included in the NBS assessment framework tool developed by the PHUSICOS project [15], as well as in the Handbook to evaluate the Impact of Nature-Based Solutions developed by [17]. Based on contextual relevance to different SES and data availability, the indicators used in each OAL are different. Given the relatively small size of most OALs, it was originally envisaged that data collection for some of the indicators would be carried out through household interviews in order to acquire data at a high spatial resolution and also to be able to quantify additional indicators, but this was not possible because of the COVID-19 pandemic. This has constrained some of our analyses (e.g., fewer indicators used), but by and large, the approach can usually be implemented without needing to collect information through household interviews. In the end, a total of 25 indicators were used and grouped into six subcomponents — ecological exposure (n = 5), social exposure (n = 3), ecosystem susceptibility (n = 3), social susceptibility (n = 5), lack of ecosystem robustness (n = 6), and lack of (social) coping capacity (n = 3) (Table 2). These sub-divisions of exposure and vulnerability follow the work by Refs. [6,9] and are taken up by Ref. [11] within the OPERANDUM project.

A spatially explicit approach was pursued in this study. However, due to the differences in study area scales (from less than 1 km^2 of OAL Austria to more than 1 thousand km^2 of OAL Italy) and data availability (e.g., paucity of spatially explicit data for the indicators) in different OALs and DCs, the calculation of the index was conducted at different scales. For OAL Italy Panaro, the final calculation of the index was conducted at the municipality scale using administrative units. For the small areas of OALs UK and Austria, and for Norwegian and French DCs, the area covered by different land-use types was treated as the spatial units for the final index calculation.

Data for all the OALs and DCs were acquired from multiple sources (Table 2). Social vulnerability indicator data were collected from census data and publicly accessible national and global repositories. Data for ecosystem indicators were calculated by combining multiple spatial datasets, such as remote sensing imagery, Corine Land Cover 2018 dataset [21], and Global Biodiversity Intactness Index [28]. The ecosystem robustness in OAL-Austria was assessed based on NDVI time series computed area-wide (spatial resolution of 10 *m*) using a stack of corrected Seninel-2 [31] imagery from 04/2017 to 01/2022. Linear trends were fitted to the NDVI values exceeding the 95% quantile in each year. The derived trends represent the evolution of the vegetation's conditions during the growing season within the considered period, with negative trends indicating stress on the ecosystem while positive trends suggest growth and robustness. Pre-processing of the data was performed using ArcGIS Pro (ESRI, Redlands, CA, USA; v. 2.8). This includes the calculation of density surfaces (e.g., density of the transportation network, population, and emergency services), spatial normalisation and zonal statistics (mean, max) to convert gridded datasets into one score for study unit within the OALs and DCs.

Table 2
Social-ecological System exposure and vulnerability indicators used in this study were selected based on the indicator library provided by Ref. [11]; indicators from the PHUSICOS project, as well as discussions with the OPERANDOM OAL partners. Vulnerability component indicators used in the assessment are arranged by sub-components (social susceptibility, social coping capacity, ecosystem susceptibility, and ecosystem robustness). Proxies were used when data for a specific indicator were not available. The column of OALs/DCs indicates what indicators the OALs/DCs used for vulnerability and risk assessment.

SES Indicators for each risk component	Proxy Taken	OALs/DCs	Data sources
Ecosystem Exposure			
EE1: Ecosystems exposed to floods (%)	N/A	Italy	Corine Land Cover 2018 dataset [21]
EE2: Proportion of agricultural land prone to flooding	N/A	Italy	Corine Land Cover 2018 dataset [21]
EE3: Proportion of the cliff prone to landslide (%)	N/A	UK	Land use map from OAL
EE4: Proportion of grassland/pasture/forest/ water bodies in flooding hazard prone area (%)	N/A	Norway	Land use map from DC
EE5: Proportion of grassland/pasture/forest/ water bodies in rockfall hazard prone area (%)	N/A	France	Land use map from DC
Social System Exposure			
SSE1: Proportion of total population exposed in hazard prone area (%)	N/A	Italy, UK	The latest available census for OALs
SSE2: Proportion of properties/buildings in hazard prone area (%)	N/A	Italy, UK, Austria, Norway, France	Properties and buildings maps from OALs/DCs
SSE3: Proportion of length of road and rail exposed in hazard prone area (%)	N/A	Italy, Austria, Norway, France	Road and rail maps from OALs/DCs
Ecosystem Susceptibility			
ES1: Normalized Difference Vegetation Index	N/A	Italy, UK, Norway, France	Cloud-free images from Landsat 8 [27] in the summer of 2018
ES2: Species richness	Biodiversity Intactness Index	Italy, UK, Austria, Norway, France	Global Biodiversity Intactness Index [28]
ES3: Freshwater scarcity	Baseline water stress (%)	Austria, Norway, France	Global Baseline water stress https://www.wri.org/applications/aqueduct/water-risk-atlas/
Social Susceptibility			
SOS1: Dependency ratio (%) includes population aged <15 yrs and >65 yrs)	N/A	Italy, Austria, Norway, France	The latest available census for OALs/DCs
SOS2: Income level (Average taxable income/ person)	N/A	Italy, Norway, France	The latest available census for OAL/DCs
SOS3: Proportion of house ownership (% of households)	N/A	Italy, Norway, France	The latest available census for OAL/DCs
SOS4: Employment rate (%)	N/A	Italy, Norway	The latest available census for OAL
SOS5: Dependency on road communication	% of people who travel to work	UK	The latest available census for OALs
Lack of Ecosystem Robustness			
ER1: Agriculture land with single or multiple crops	% agriculture land with single or multiple crops	Italy	Statistic yearbook from AOL
ER2: Mean Species Abundance	N/A	Italy, UK, Austria, Norway, France	Global patterns in mean species abundance (MSA) values [29]
ER3: Landscape fragmentation	Landscape Aggregation Index	Italy, UK, Norway, France	Calculated combing Fragstats software [30] and Corine Land Cover 2018 dataset [21]
ER4: Lack of Policies supporting biodiversity conservation (yes/no)	N/A	Italy	Policy review for OAL
ER5: Lack of Policies for forest/grassland conservation (yes/no)	N/A	Austria, Norway, France	Policy review for OAL
ER6: Lack of Policies for coastal protection (yes/ no	N/A	UK	Policy review for OAL
ER7: Evolution of vegetation productivity	N/A	Austria	Time series of Sentinel-2AB imagery from 04/ 2017 to 01/2022
Lack of coping and adaptive capacity			
CAC1: Access to transportation network	The density of the transportation network (road length per 1000 population)	Italy	The latest available census for OAL
CAC2: Vehicles	Number of cars per person	Italy	The latest available census for OAL
CAC3: Existence of adaptation policies/strategies (yes/no)	N/A	Italy, UK, Austria, Norway, France	Policy review for OALs and DCs

3.3. Vulnerability and risk assessment for the OALs and DCs

Following previous SES vulnerability and risk assessment workflows [7,8], data pre-processing for indicators included detecting and treating outliers and multicollinearity. The potential outliers in the data were examined using both box plots based on the interquartile range - IQR (i.e., data outside $1.5 \times$ IQR), skewness and kurtosis of the data (i.e., skewness greater than 1 or smaller than -1, and kurtosis greater than 3.5). Triangulation was used to verify potential outliers, and a winsorization approach was used to treat

the outliers, i.e., by an iterative replacement of the highest/lowest with the second-highest/lowest indicator scores – an approach that has been used in SES index construction (e.g., Refs. [7,8]). Two indicators (i.e., employment rate and access to transportation network) for OAL Italy Panaro, three indicators (i.e., NDVI, Species Richness and Mean Species Abundance) for Norwegian DC, and two indicators (i.e., Mean Species Abundance and Landscape Fragmentation) for French DC were treated using winsorization (Table S1).

Multicollinearities within each of the four vulnerability domains were assessed using correlation matrices (Kendall's Tau) and variance inflation factor (VIF). Statistical significance was tested using a two-tailed approach. Following this approach, no indicators were excluded as there were no correlations of $r > 0.90$ ($p < 0.05$) for all the OALs. For PHUSICOS DCs, multicollinearity was detected for all social susceptibility indicators, so they were all excluded except for the dependency ratio.

Because many indicators had skewed distributions and varying ranges, as well as the difficulties associated with defining standardisation thresholds, the min-max standardisation method was applied to rescale the indicators to a range between zero and one [32]. Indicators with high scores contributing to reduced vulnerability and risk were inverted during the normalisation process so that all higher values equated to higher vulnerability.

The equally weighted ($w_i = 1$) standardized indicators (x_i') were combined into the four vulnerability domains (*VD*; i.e., ecosystem susceptibility, social susceptibility, lack of ecosystem robustness, and lack of coping/adaptive capacities) using additive aggregation (Eq. (1)) [7].

$$VD = \sum_{i=1}^{n} \left(w_i \times x_i' \right)$$

The ecosystem susceptibility and social susceptibility were aggregated into a metric representing SES susceptibility, while the lack of ecosystem robustness and lack of coping/adaptive capacities were combined into a metric representing the lack of capacities/robustness of the SES (Eq. (2)) to calculate vulnerability domains of the SES (VD_{SES}) [7]. Equal weights are applied in all cases.

$$VD_{SES} = \sum_{j=1}^{n} \left(w_i \times VD_j \right)$$

Finally, the vulnerability of the SES (VU_{SES}) was calculated by using the average of the susceptibility of the SES (VD_{SUS}) and the lack of capacities and robustness of the SES (VD_{LCR}) (Eq. (3)) [7].

$$VU_{SES} = \frac{VD_{SUS} + VD_{LCR}}{2}$$

Exposure of the SES to a single hazard (i.e., flood in OAL Italy and Norwegian DC, landslides in OAL Austria and the UK, and rockfall in French DC) was assessed by calculating the average percentage of both ecological and social components (see Table 2 and Data 1) in hazard-prone areas using gridded data and a spatially explicit approach in a GIS. Hazard scores refer to spatial flood or landslide magnitude within the OALs and DCs units based on the modelling results from other work packages of OPERANDUM and PHUSICOS [33]; [34]. For OAL Italy Panaro, the hazard score was calculated based on the flood depth within the region of the municipality. In particular, we referred to maximum water depths reproduced by means of a 2D hydraulic model (developed using HEC-RAS software; USACE, 2020), which simulated water dynamics in case of flood inundation in the study area. For the OAL-UK, the hazard score was calculated based on the Factor of Safety (FoS [35]; upon which slope stability was evaluated at a soil depth of 200 mm below ground level modelled with a modified version of the process-based model Plant-Best [25], while for OAL Austria, the hazard score was calculated based on the landslide velocity [36] [22],). Similarly, for Norwegian DC the hazard score was calculated based on the maximum flood depth which occurred at each cell of the volume conservation flood routing model extended to the study area, developed using FLO-2D software [37]. For the French DC, the hazard score was assessed considering the product of maximum rockfall energy and reach probability. For both PHUSICOS DCs, the min-max method was applied to standardize hazard scores. It should be noted that to render the datasets comparable, the lowest min or highest max values under different scenarios (e.g., with/without NBS implementation) were used in the normalisation process for exposure scores (EXP_{SES}) and hazard scores (HAZ_{SES}) and then yielded the final risk-comparable scores ($RISK_{SES}$) (Eq. (4)).

$$RISK_{SES} = EXP_{SES} \times HAZ_{SES} \times VU_{SES}$$

All vulnerability, exposure and risk outputs are mapped based on a quantile classification following previous SES risk assessment studies [7,8]. The relative scores were classified as Low, Medium Low, Medium, Medium High, and High vulnerabilities or risks. For Norwegian DC, vulnerability and exposure are mapped on a natural break classification to enhance data visualization.

3.4. Risk calculation under NBS implementation scenarios

This study selects OAL Italy Panaro and OAL UK as well as the Norwegian and French DCs as the cases to calculate the risk under the NBS implementation scenarios based on data availability. The OAL Austria was not considered for calculation of risk under NBS implementation scenario as the modelling study was still on-going at the time of writing.

For OAL Italy, the vulnerability was held at the same levels for the two scenarios, and changes in risks were computed by considering the effects of hazard and exposure components which are related to the flood extent (used to derive exposure) and flood depths of inundated regions (i.e., hazard score). The flood extents and depths under the with/without NBS implementation scenarios were modelled under the 200-year flood event by the other work package of the OPERADUM project (e.g., Ref. [33]). This allowed us to de-

termine flood hazard and exposure reduction effects of the NBS and assess changes in risk per municipality. Flood hazard characteristics maps with/without NBS implementation scenarios were overlain on the same map of land use types, population, buildings, and road and rail for modelling the exposure components to calculate ecological and social exposure. We first present social and ecosystem exposure changes and hazard components with and without NBS scenarios. We also show changes in the risk as a result of the NBS using social and ecosystem risk class changes per municipality.

For the OAL UK, the vulnerability was held at the same levels for different implementation scenarios, and changes in risks were computed by considering the effects of hazard and exposure components which are related to landslide-prone regions (used to derive exposure) and reverse of Factor of Safety (FoS) (i.e., hazard score). The landslide hazard score under the with NBS (maple and willow planting) and without NBS (fallow) implementation scenarios were modelled under baseline condition for the year 2011 and under climate change scenario Representative Concentration Pathway (RCP) 4.5 for the year 2073. We took 2011 as the baseline year because this was the year in which the meteorological station was deployed at the OAL-UK. This was prior to the occurrence of major landslide events at the OAL in 2012 and prior to the implementation of any NBS from 2013 on. This allowed us to determine landslide hazard and exposure reduction effects of the NBS and assess changes in risk per grid in the landslide-prone regions in the OAL UK. The performance of the considered NBS (i.e., high-density planting) against landslides at OAL UK was modelled with a debugged version of the Plant-Best model [25].

In Norwegian and French DCs, and similarly to OAL Italy, vulnerability was kept constant for both the with/without NBS implementation scenarios and variations in risk scores depended on changes in hazard and exposure values which are related to hazard extent and intensity. In detail, for Norwegian DC, the flooding extent and maximum depth were simulated, during other PHUSICOS project activities, under a 200-year event occurring in the most severe baseline scenario, i.e., when the culvert is totally obstructed, and in the NBS scenario, i.e., when the pipeline is replaced with the open watercourse. The flood extent was adopted for exposure indicators assessment while an area-weighted maximum flood depth was assigned to each land use class in the study area. For French DC, the rockfall hazard extents and intensity under the baseline scenario (i.e., current situation) and NBS scenario (i.e., wooden tripods, meshes and barriers implemented) were simulated under a 100-year return period rockfall event, with 1 m^3 volume boulders, as achieved in another work package of the PHUSICOS project. Rockfall prone areas extension was used for the evaluation of exposure indicators while an area-weighted rockfall hazard score, resulting from the product of standardized maximum kinetic energy and reach probability maps, was associated to each land use class in the study area.

4. Results

4.1. Vulnerability and risk assessment in the context of NBS for flooding: a case study in Italy

4.1.1. SES vulnerability to flooding in OAL Italy panaro

SES vulnerability to flooding in OAL Italy is calculated for present baseline conditions only, irrespective of hazard and NBS project implementation scenarios. Based on the available data for selected indicators used for computing the vulnerability, the overall score for SES vulnerability to flooding in OAL Italy shows that municipalities in the southeastern region along the Panaro river are more vulnerable than other municipalities (Fig. 4). This is essentially due to higher SES susceptibility scores linked to land covered with vegetation (ES1), biodiversity intactness (ES2), house ownership (SOS3) and employment rate (SOS4).

4.1.2. Hazard and exposure without and with NBS implementation scenarios in OAL Italy panaro

Flood hazard is quantified as the flood depth expected at each municipality for the two river configurations (i.e., without and with NBS) in case of the occurrence of a 200-year flood event along the Panaro river. The proposed NBS aims to strengthen the embankment, thus limiting the triggering of failure mechanisms. The capability of the NBS (i.e., deep root plants) to completely avoid the toe erosion process, as well as the superficial erosion of the levee in case of its overtopping, is still to be proven; nevertheless, this study builds upon such hypothesis and evaluates the expected benefits assuming mature NBS implementation and performance. Thus, the two adopted river configurations are: i) current levee design (without NBS), which is expected to collapse in case of overtopping; ii) NBS in place, which assumes that the complete collapse of the levee once overtopped is prevented by the NBS.

Hydraulic simulations carried out on the OAL Italy for the specific flood scenario show that mainly the south-eastern municipalities are affected by flooding under both configurations (hazard score >0.5; Fig. 5). However, flood depths are expected to be significantly reduced in case of NBS implementation (Fig. 5) thanks to limited overflow associated to the configuration with NBS. The total flooded area in OAL Italy could be reduced by 40.6% (from 120.98 km^2 to 71.85 km^2), thanks to the implementation of the NBS project.

Exposures of the social and ecological components are assessed within the flood hazard-affected area in OAL Italy Panaro. Exposure score maps for both ecosystems and social systems show that southern municipalities have higher ecological and social exposures under both scenarios (with and without NBS) (Fig. 6). Here, we estimated ecosystem exposure based on two indicators – the proportion of ecosystems exposed to flooding (EE1) and proportion of agriculture land prone to flooding (EE2). We estimated social exposure based on three indicators – the proportion of the population (SSE1), the proportion of buildings (SSE2), and the proportion of railroads (SSE3). As the NBS implementation is expected to reduce the extent and depth of flooding, it will eventually reduce social and ecological exposure in flood-affected areas. Therefore, for both ecosystem and social systems, the results show that some municipalities with 'High' exposure scores under the without NBS scenario will have 'Medium high' to 'Medium' exposure scores under the with NBS scenario (Fig. 6). Similar results are found for the combined score for SES exposure, but we observe a slightly higher score in the southernmost municipality. This is because the hazard score was calculated based on the flood depth within the area of the municipality, while the exposure of the SES to a single hazard (i.e., flood in OAL Italy Panaro) was assessed by calculating the average per-

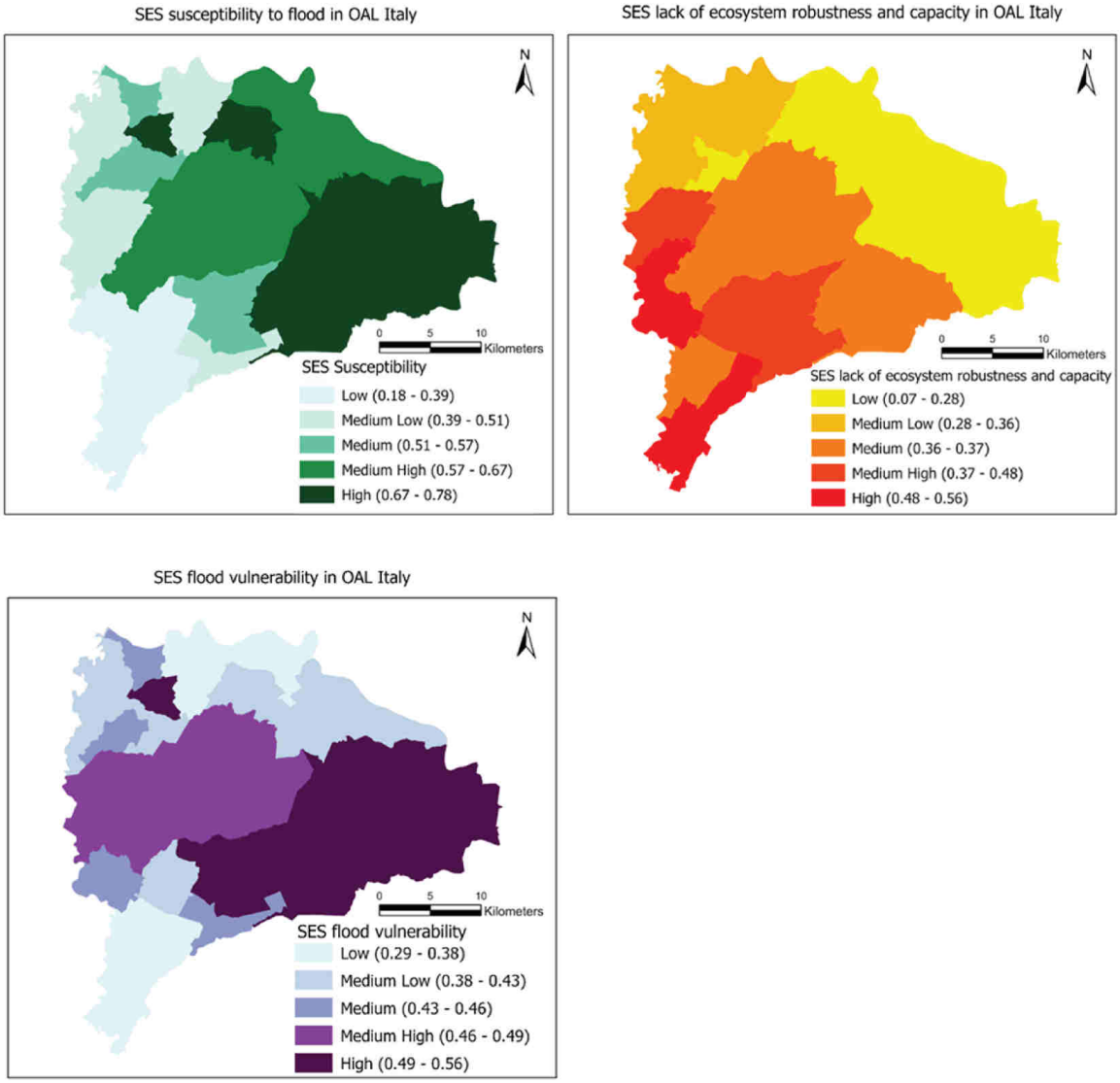

Fig. 4. Social-ecological System (SES) social and ecological susceptibilities (upper left), lack of ecosystem robustness and social coping capacity (upper right) and final SES vulnerability (bottom) with respect to floods in OAL Italy.

centage of both ecological and social components in hazard-prone areas using gridded data and a spatially explicit approach in GIS. Although the total exposure area in Panaro reduces from 119.28 km^2 to 70.13 km^2, for Bomporto (the southeast municipality), the exposure areas of this south-eastern region increase from 16.41 km^2 to 18.16 km^2 between without and with NBS scenarios (Fig. 6). There is a greater population density, building area and road length; therefore, although the ecosystem exposure score reduces from 0.89 to 0.85, the social exposure score increases from 0.66 to 0.73 and as a consequence, the SES-exposure score increases from 0.78 to 0.79, between without and with NBS scenarios.

4.1.3. Risk assessment in OAL Italy Panaro

SES risk scores for OAL Italy Panaro under without-NBS scenario show that the southern municipalities have a high risk of flooding (risk score - Medium-high to High (0.168–0.354)), particularly in the mid-southern region along the Panaro river (Fig. 7), which is logical as the SES exposure and vulnerability scores are higher for this region. However, implementing NBS will reduce risk levels for all high-risk areas to medium risk (score: 0.032–0.168). In addition, some Medium-high and Medium risk areas will see their risk levels reduced, thanks to NBS implementation (Fig. 7). Overall, mean risk scores for all municipalities under the without-NBS scenario will be decreased by 60% under the NBS scenario (Table 3).

Flood depth will decrease by around 27% when the NBS is implemented (from 1.02 *m* to 0.74 *m*), which will reduce ecosystem-exposed areas by 40.6%, agriculture-exposed area by 38.8%, population exposure by 53.0%, building exposed area by 58.5%, and road and rail infrastructure exposure by 39.8% under 'with NBS' scenario (Table 3).

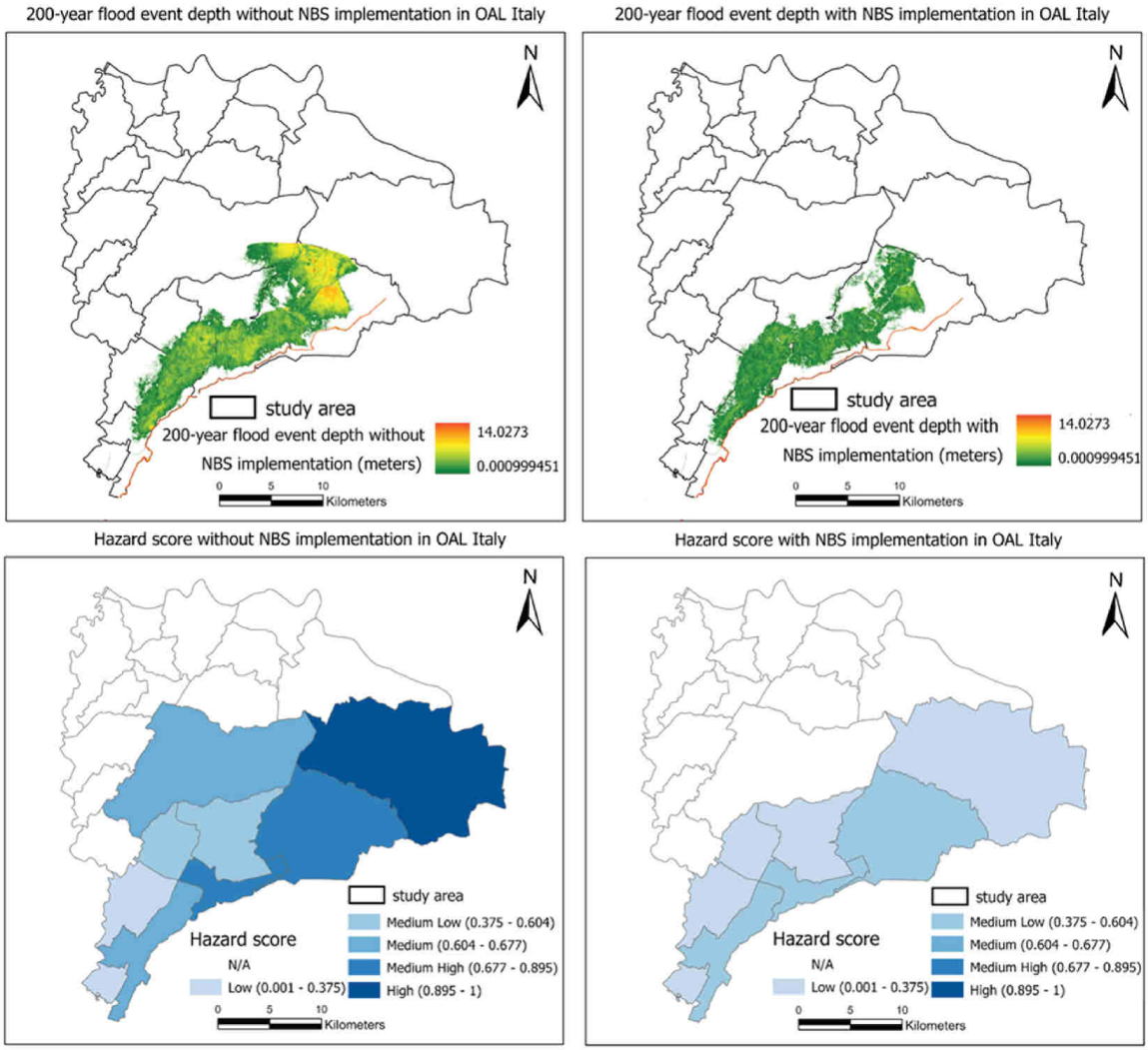

Fig. 5. Extent, magnitude, and hazard scores of flooding for a 200-year flood event in the OAL Italy in case of levee failure (without NBS; left panels) and controlled overtopping (with NBS, right panels) configurations.

4.2. Vulnerability and risk assessment in the context of NBS for landslide: a case study in the UK

4.2.1. SES vulnerability for landslide in OAL UK

The results show that around 80% of the OAL UK area has an SES vulnerability score ranging from Low to Medium. Higher SES vulnerability scores (Medium-high to High; Fig. 8) are in the residential and infrastructure land use areas where houses, population and roads are located, as well as in the water bodies where the landscape aggregation index is high. Spatial variation of SES vulnerability scores in OAL UK is mainly influenced by land use types. 'Building' type land use, which are concentrated in small areas, show little variation of vulnerability score within that land use area, whereas other land uses (e.g., forest, farmland, river), which cover larger areas, show wide variations of vulnerability scores within those land use boundaries.

4.2.2. Hazard and exposure without and with NBS implementation scenarios in OAL UK

OAL UK is located along a coastal slope that is prone to landslides. Landslide-prone zones were detected using the Plant-Best model and associated landslide detection module [25,38] under three land cover scenarios, i.e., fallow, willow, and maple, and under current (2011) and future climate scenarios (i.e., 2073; RCP 4.5). Willow and maple scenarios refer to the utilisation of high-density planting as an NBS for landslides. Zones were classified as prone to landslides when FoS was below 1.3. The FoS was calculated using the limit equilibrium method embedded in the Plant-Best model [25]. The simulation output indicated that high-density planting as NBS has a positive effect against landslides. As per the baseline estimate for the year 2011, around 8.23% of the OAL's area was prone to landslides. Under fallow ground in 2011, ca. 7% of landslide prone zone had a Medium hazard score, while the rest of the landslide-prone zone (93%) had a Low to Medium-Low hazard score. Zones with Medium-High to High hazard score were not identified under the 2011 fallow cover. Estimates of the hazard score with NBS (i.e., High-density Maple and Willow plantation) for the year 2011 suggested that the NBS can reduce the landslide hazard, decreasing the score to the Low range for the whole landslide prone zone (Fig. 8).

Under future climate change conditions (RCP 4.5, Fig. 8), it is estimated that in 2073, without NBS (i.e., fallow ground), between 15.36% and 19.37% of the landslide-prone zones had Medium-High SES and High hazard scores, respectively (Fig. 9). However, with

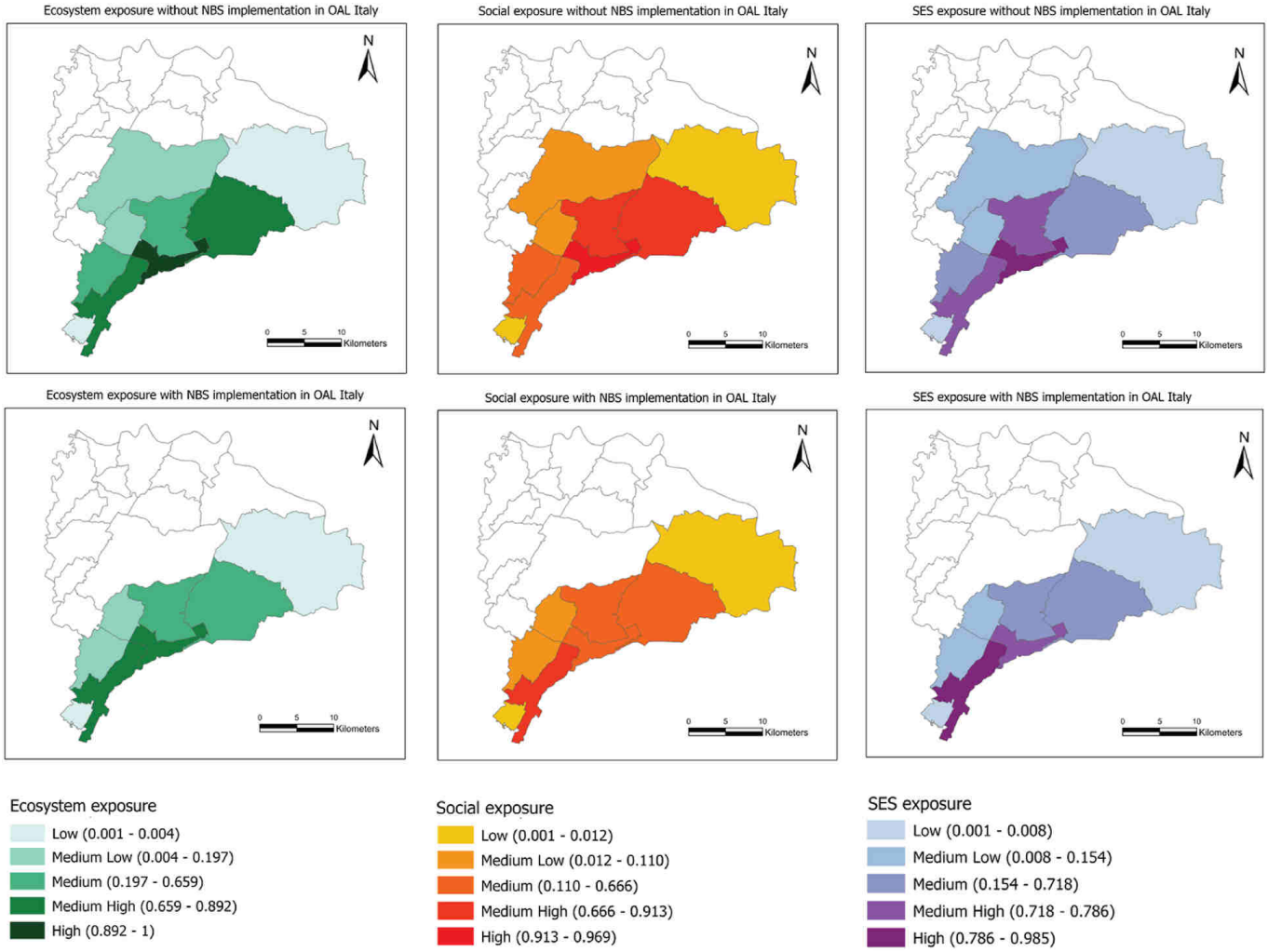

Fig. 6. Ecosystem exposures, social exposures, and the SES exposures in OAL Italy under with (bottom panels) and without (upper panels) NBS scenarios.

NBS, the hazard scores were much lower than the fallow ground cover under future climate scenario. Under maple plantation in high density, between 8.23% and 16.74% of the landslide-prone areas had Medium-High and High hazard scores, respectively. Under willow plantation, from 1.03% to 1.25% of the landslide-prone areas resulted in Medium-High and High hazard scores, respectively (Figs. 8 and 9).

SES exposure is defined by land use types in OAL UK. Since all the SES elements are exposed to landslides in this small area, we could not calculate spatially differentiated exposure scores within the OAL. So, we considered the SES exposure value equal to 1 for all land use types.

4.2.3. Risk assessment in OAL-UK

Under current climate conditions and without the NBS (i.e., fallow), landslide-prone areas (Medium-high SES and High SES risk score zones) represented ca. 14.82% of the area (Fig. 10). However, with NBS (i.e., maple and willow plantation in high-density on landslide-prone zones), the area of landslide-prone zones (Medium-high SES and High SES risk score zones) decreased to 13.06% and 14.35%, under maple and willow plantation, respectively. Under future climate change scenario (i.e., 2073 RCP 4.5), without NBS between 13.18% and 15.28% of the landslide-prone areas had Medium-high and High SES risk scores, respectively. However, with NBS, the SES risks were lower than without NBS. Under maple plantation, between 7.83% and 7.9% of the landslide-prone areas resulted in Medium-High and High SES risk scores, respectively. Under willow plantation, 1.20% and 11.68% of the landslide-prone areas resulted in Medium-High and High SES risk scores, respectively (Figs. 8 and 9).

4.3. Vulnerability and risk assessment in the context of NBS for a deep-seated landslide: a case study in Austria

4.3.1. SES susceptibility and vulnerability for landslide in OAL Austria

In OAL Austria, the SES susceptibility to landslide movement is high throughout the actively moving landslide in the entire OAL. The SES vulnerability to the landslide is generally high in the settlement in the central part of the active landslide (score: Medium-high to High), covering around 5% of the area (Fig. 11). Around 43% of the area has medium SES vulnerability to the landslide's movement, including mostly forested areas. Mainly houses/infrastructure fall within the Medium to High susceptibility range. Similar to OAL UK, spatial variation of SES vulnerability in OAL Austria is also influenced by land use type. All land use types, except residen-

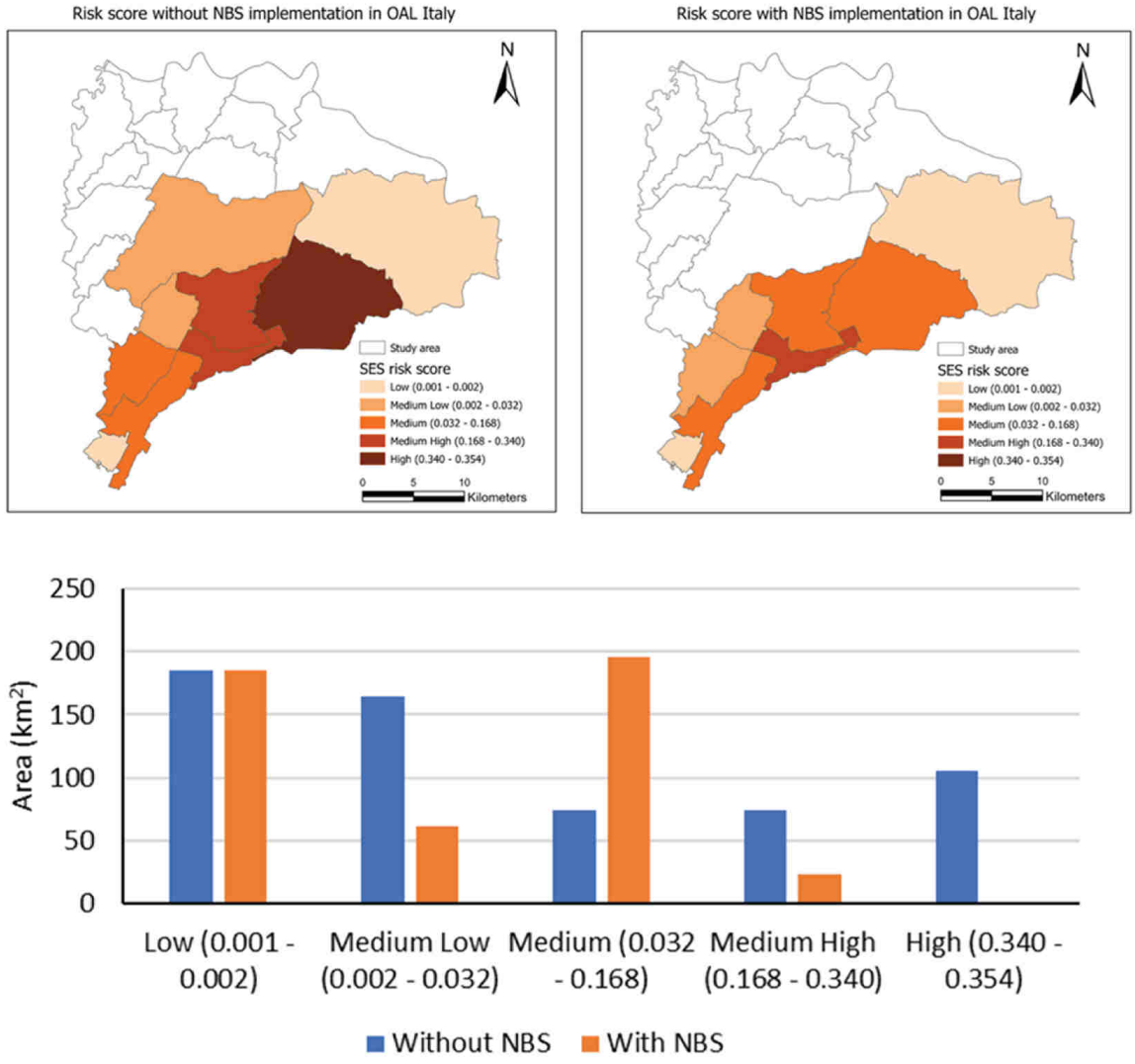

Fig. 7. SES risk scores for a 200-year flood event in OAL Italy under with-NBS (upper right) and without-NBS (upper left) scenarios, and area in different SES risk levels in OAL Italy under with-NBS and without-NBS scenarios (bottom).

Table 3
Comparison of exposure and risk-related data under the without-NBS implementation scenario with corresponding data under the with-NBS implementation scenario.

	Without NBS	With NBS	Change (%)
Flood depth (m)	1.02	0.74	−27.45
Ecosystem exposed to flooding (km^2)	120.98	71.85	−40.61
Agriculture area exposed to flooding (km^2)	112.15	68.67	−38.77
Population exposed to flooding (count)	7865	3688	−53.11
Properties/buildings exposed to flooding (km^2)	1.11	0.46	−58.56
Length of road and rail exposed to flooding (km)	350.55	211.08	−39.79
Mean ecosystem exposure score for 22 municipalities	0.17	0.14	−17.65
Mean social exposure score for 22 municipalities	0.17	0.09	−47.06
Mean SES exposure for 22 municipalities	0.17	0.12	−29.41
Mean hazard score for 22 municipalities	0.26	0.13	−50.00
Mean Risk score for 22 municipalities	0.05	0.02	−60.00

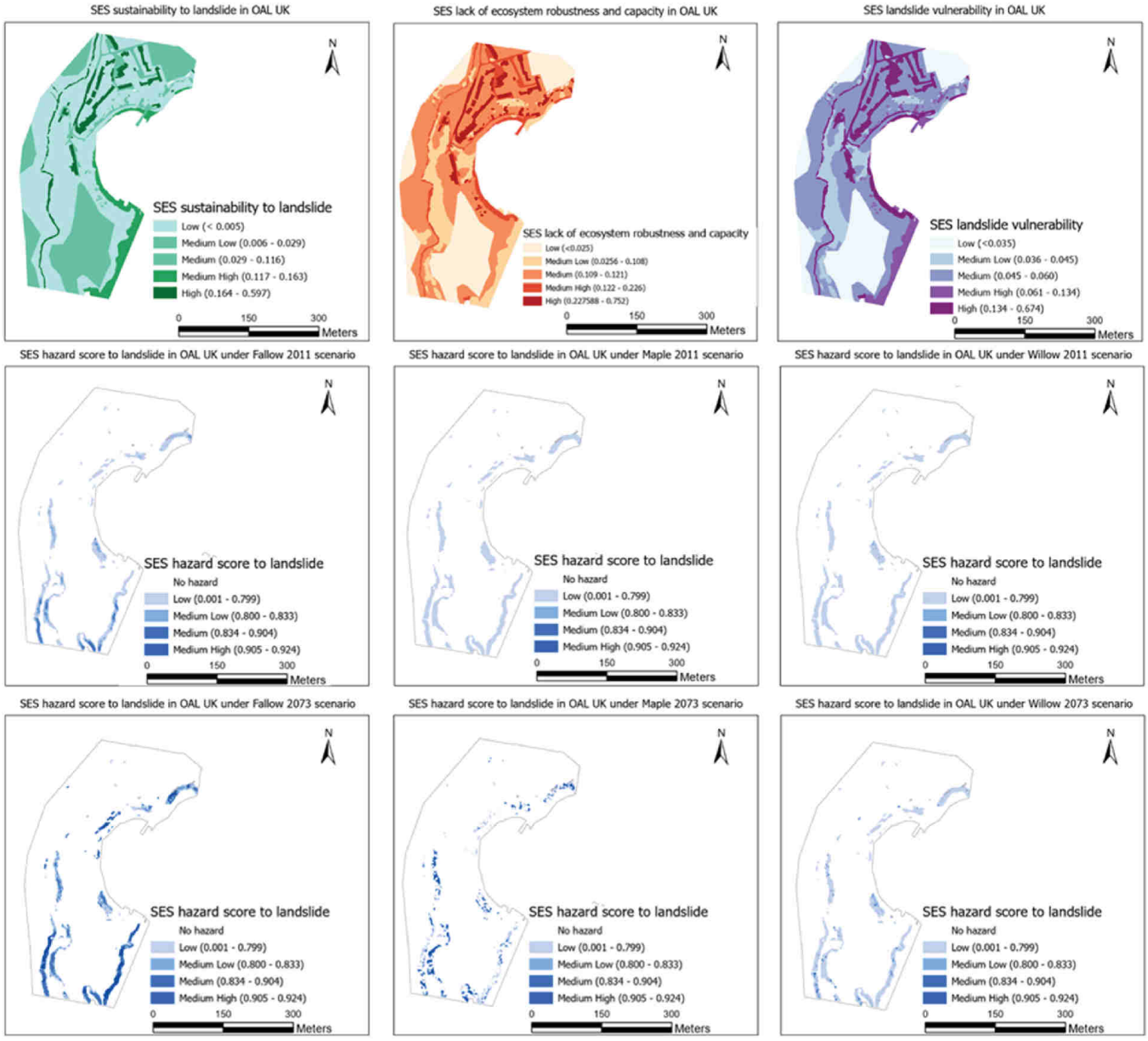

Fig. 8. Social and ecological susceptibilities; lack of ecosystem robustness and lack of social coping capacities; and vulnerability (top three figures from left to right, respectively) and landslide hazard scores (remaining six figures) with NBS implementations (maple and willow planting) and without (fallow) NBS implementation under the climate change scenario RCP 4.5 for the years 2011 and 2073 in OAL UK.

tial or infrastructure, show a significant variation of vulnerability score within those land use boundaries. The ecosystem robustness of the forest areas in the northern part of the landslide is considered high, as these areas show a positive NDVI trend for the past five years. Mainly the ecosystems in the vicinity of the settlement and the agricultural areas lack robustness in recent years.

4.3.2. Hazard and exposure in OAL Austria

The main hazard in OAL Austria is the internal deformation of the landslide body and the related damage to brittle structures on top of it (e.g., buildings and roads), due to comparably high landslide velocity (>5cm/a) and/or differential displacements within the contact zone of landslide sub-units. Based on these criteria, our estimates show that a large part of OAL Austria (64%) falls under a high hazard score (1.0) and the rest of the area falls under a lower hazard score (0.5) (Fig. 11). Similar to OAL UK, SES exposure is defined by land use types. Since the OAL area is very small and all the SES elements are exposed to the landslide, we considered the SES exposure value equal to 1 for all land use types.

4.3.3. Risk assessment in OAL Austria

In OAL Austria, at present scenario without NBS, mainly buildings and roads fall within the Medium-High to High risk areas, which cover around 3% of the area located in the central part (Fig. 11). The houses and other buildings mainly fall within the High-risk area. Medium-low and Medium risk areas are in the north-eastern part, mainly dominated by forests (Fig. 11). The lowest risk scores were obtained for agricultural areas which are the least affected by the landslide. We did not investigate the potential SES risks

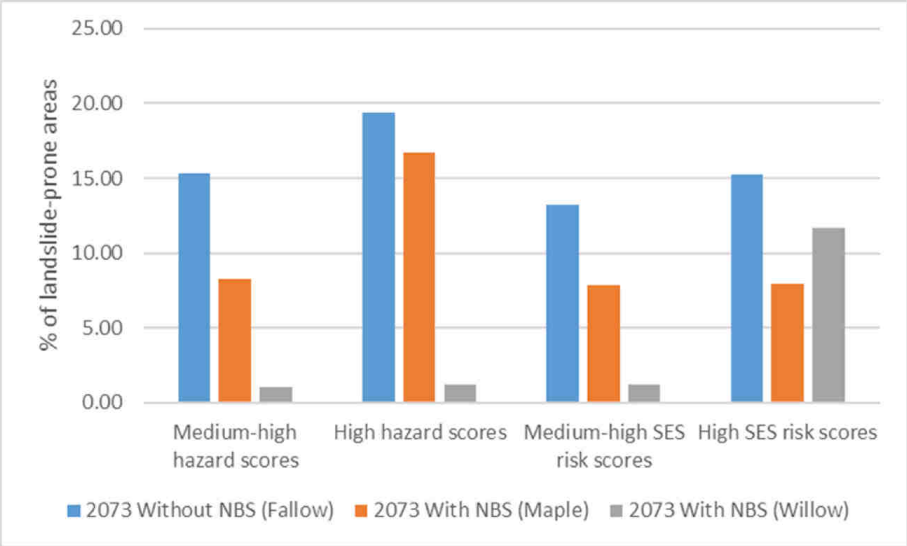

Fig. 9. Percentage of landslide-prone areas with Medium-High and High hazard and risk levels in OAL UK under NBS (Maple and Willow) and no-NBS (Fallow) scenarios under climate change conditions (i.e., 2073; RCP 4.5).

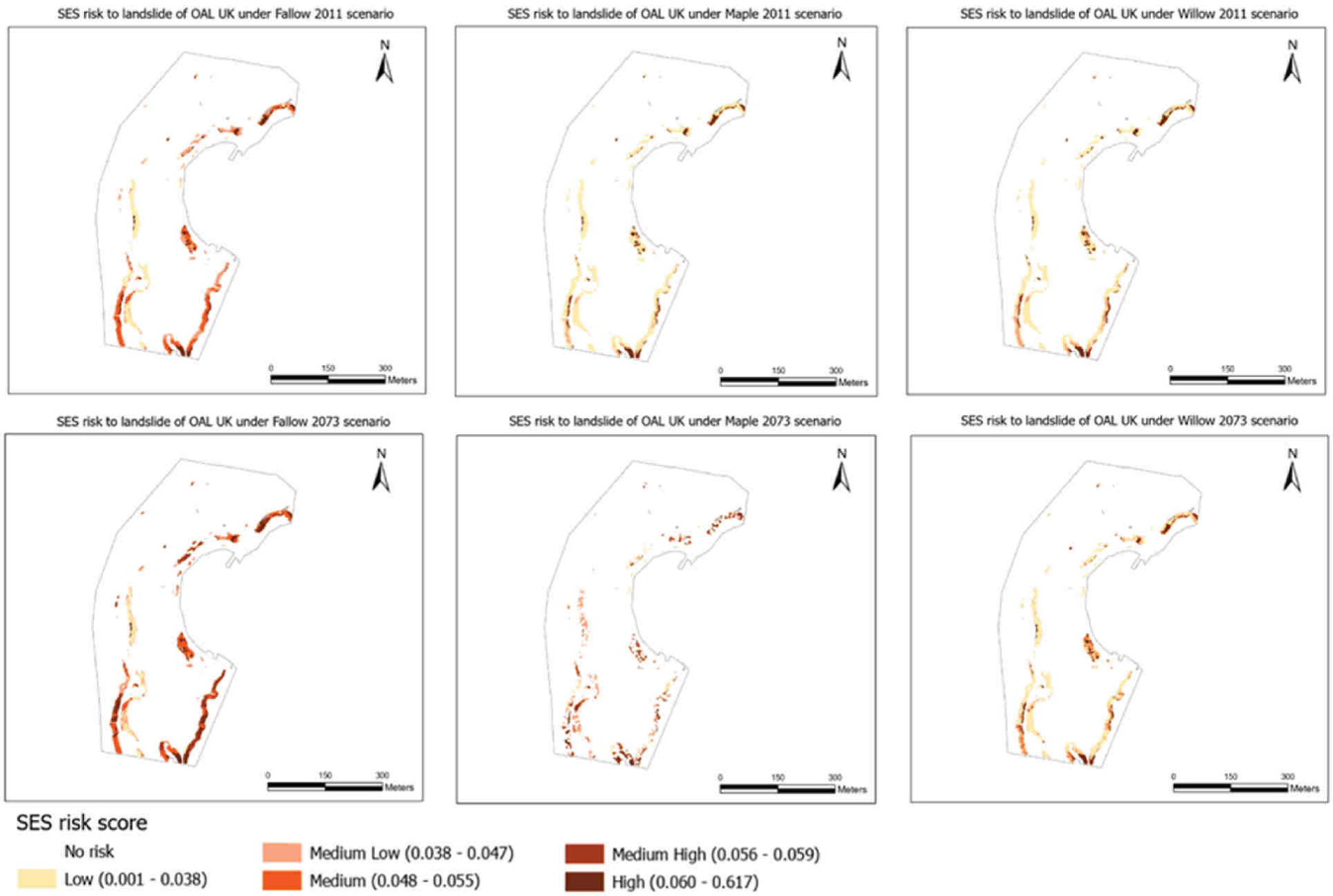

Fig. 10. SES risk scores with NBS implementations (Maple and Willow planting) and without (fallow) NBS implementation under the climate change scenario RCP 4.5 for the years 2011 and 2073 in OAL UK.

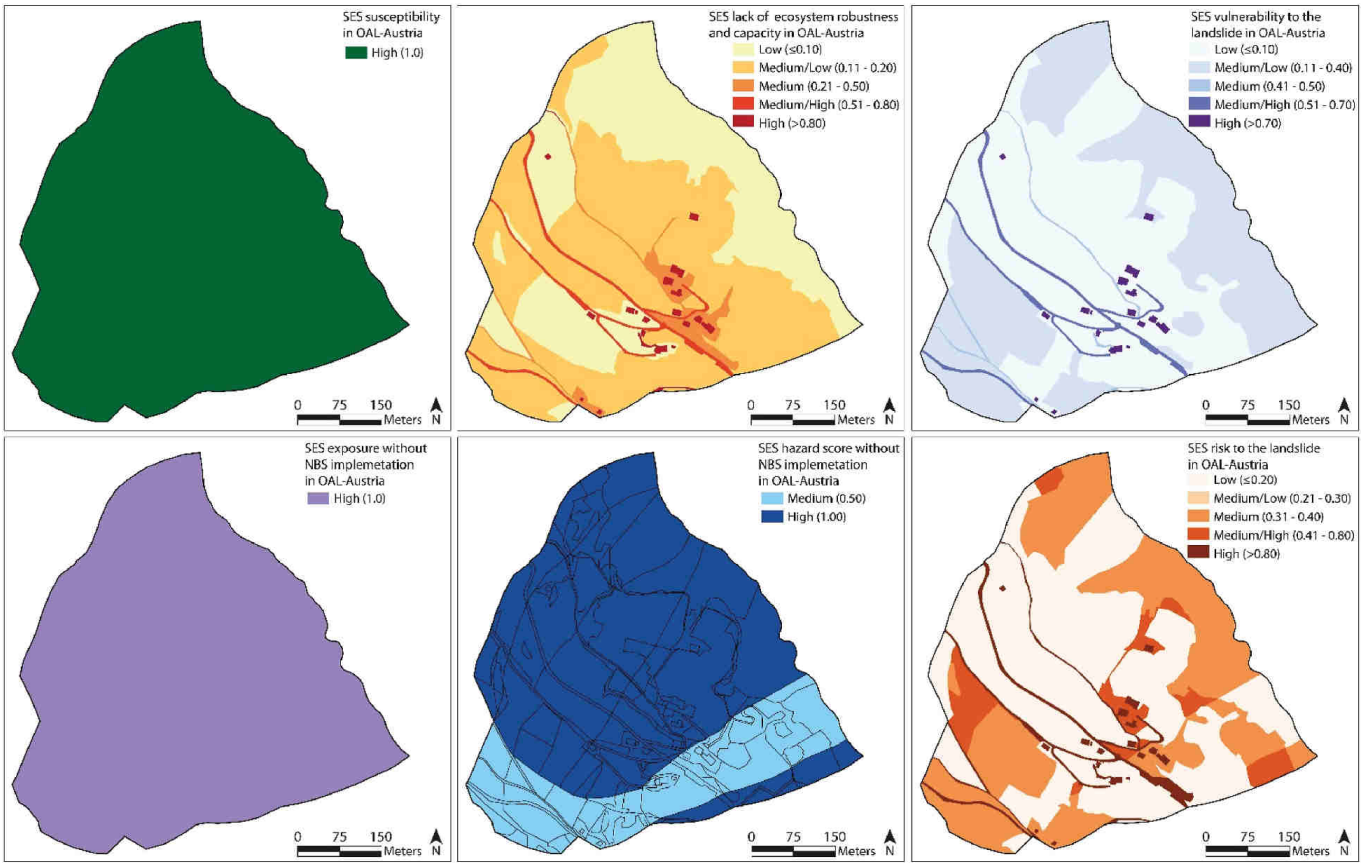

Fig. 11. SES susceptibility (top-left), lack of ecosystem robustness (top middle), vulnerability (top right), exposure (bottom left), hazard (bottom middle) and risk (bottom right) in OAL Austria.

under 'with NBS' scenario yet due to lack of data. It could be explored in the future when more data on NBS implementation will be available.

4.4. Vulnerability and risk assessment in the context of NBS for flooding: PHUSICOS case study in Norway

4.4.1. SES vulnerability to flooding in PHUSICOS Norwegian DC – Øyer

In Norwegian DC, SES vulnerability to flooding is estimated for current baseline conditions only, since NBS project implementation will not affect it. According to selected indicators applied for assessing the vulnerability, the overall score for SES vulnerability to flooding in Norwegian DC shows that the most vulnerable areas are those in between the two main roads and in the upper part of the study area (Fig. 12). This is mainly due to higher SES susceptibility scores, linked to land covered with poor vegetation (ES1), and to higher SES lack of ecosystem robustness and capacity because of low mean species abundance (ER2) and relevant landscape fragmentation (ER3).

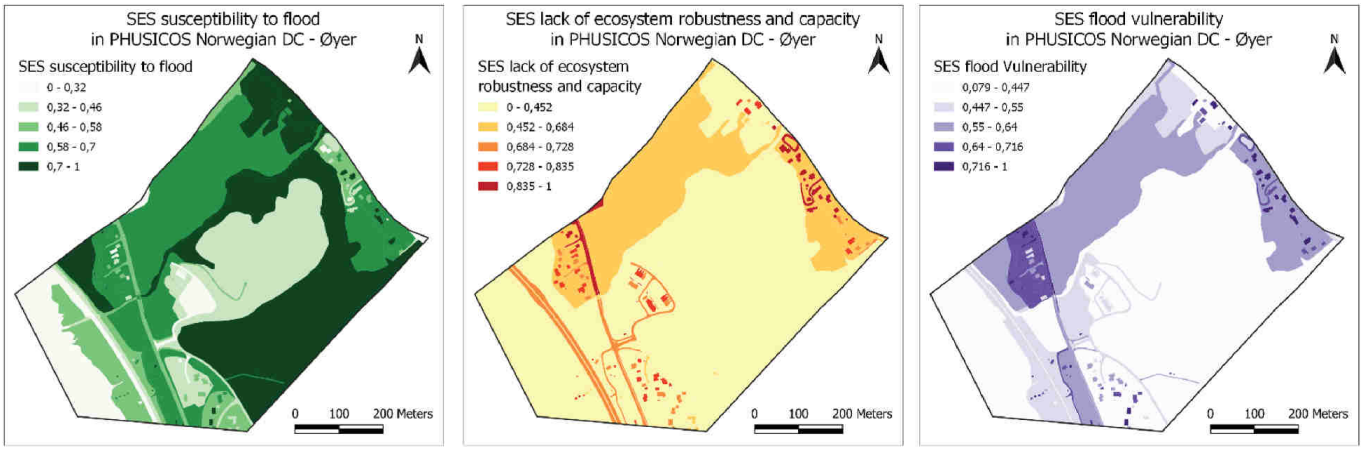

Fig. 12. Social-ecological System (SES) susceptibility (left), lack of ecosystem robustness and capacity (central panel) and final SES vulnerability (right) with respect to floods in PHUSICOS Norwegian DC.

4.4.2. Hazard and exposure without and with NBS implementation scenarios in PHUSICOS Norwegian DC – Øyer

Flood hazard is quantified as the maximum flood depth expected at each cell of the study area grid ($2\,m \times 2\,m$), for both the baseline and NBS scenario configurations (e.g., without and with NBS) in case of occurrence of a 200-year flood event along the river Søre Brynsåa and the Todalsbekken creek. The NBS is aimed to replace a 600 mm diameter pipeline with an open watercourse to enhance its capacity during floods. Therefore, the two adopted river configurations are: i) current situation (without NBS), which is expected to experience an inundation of the two major roads and the area in between and threaten the surrounding dwellings when the culvert is obstructed; ii) NBS in place, which should prevent the inundation by keeping the water inside the open creek bed.

Hydraulic simulations were carried out on Norwegian DC using the methodological framework adopted in previous PHUSICOS work packages [39]. Since the hydraulic model chosen to simulate flooding, namely FLO-2D, is a volume conservation flood routing model, its main uncertainties are linked to volume conservation, i.e. the difference between the total inflow volume and the outflow volume plus the storage and losses, which is an indication of numerical stability and accuracy. Moreover, the model could suffer from some uncertainties related to how detailed hydrologic, topographical and land use input data are. With regard to Norwegian DC, the model input data, i.e., the soil curve number and the hydrographs, were developed using, respectively, high resolution data achieved by Norwegian Mapping Authority [40], and Intensity-Duration-Frequency (IDF) curves, estimated by processing, IDF values provided by the Norwegian Centre for Climate Services (NCCS) for Lillehammer station, located 15 km far from Øyer, considering 23 seasons, from 1969 to 1991, with reference to a 200 years return period. During hydraulic simulations an acceptable level of error in the volume conservation, within 0.001%, was achieved [37].

The outputs for a 200-year event in the current condition show how, if the culvert is obstructed, both the Søre Brynsåa and the Todalsbekken overflow and threatens the main roads and the areas surrounding the creek beds (hazard score <0.5; Fig. 13). When the

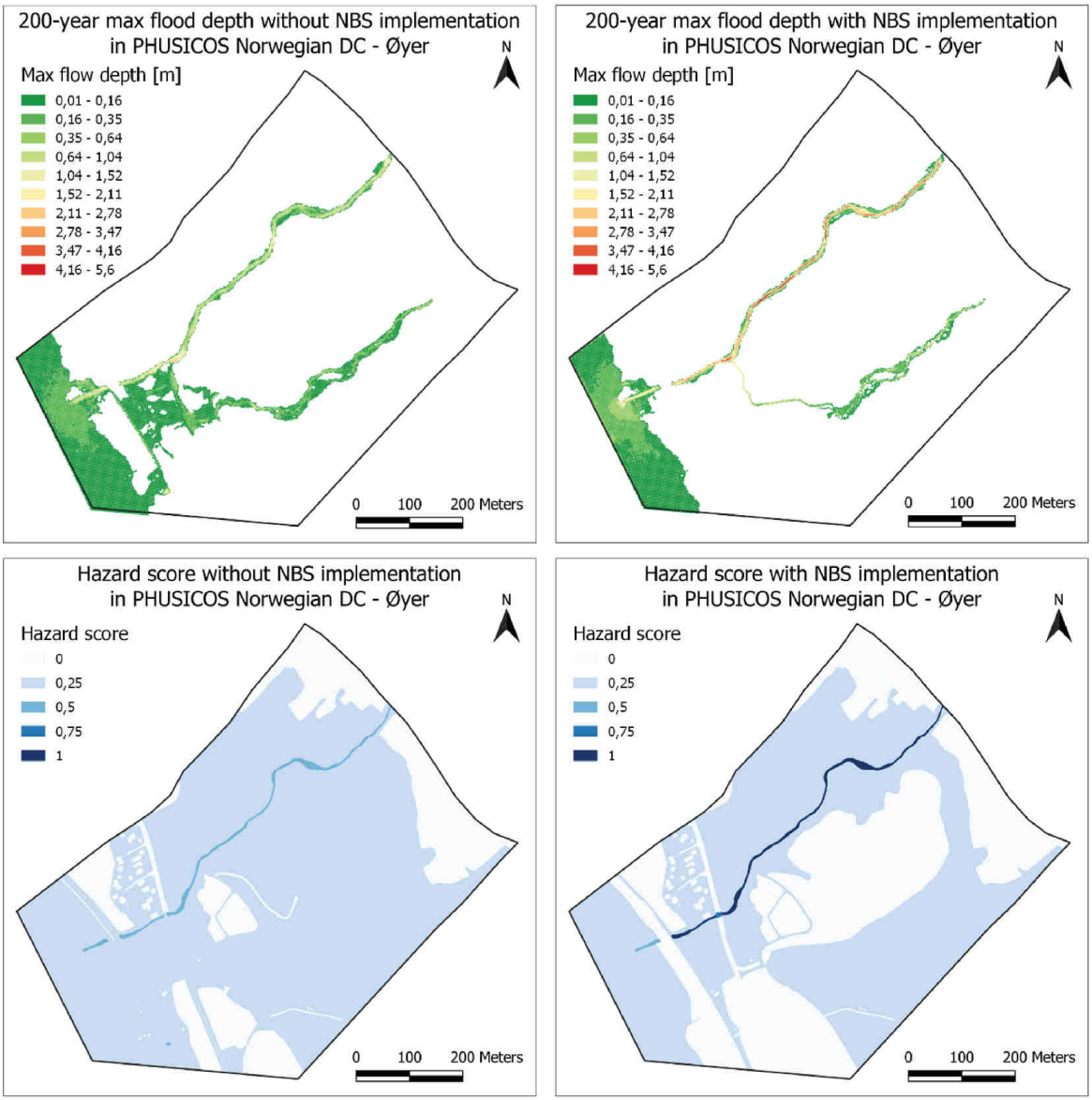

Fig. 13. Extent, magnitude and hazard scores of flooding for a 200-year flood event in the Norwegian DC in case of culvert obstruction (without NBS; left panels) and open watercourse (with NBS, right panels) configurations.

NBS is implemented, maximum flood depths are expected to be significantly reduced, especially along the Todalsbekken creek (Fig. 13). NBS project implementation could potentially induce a beneficial reduction of total flooded area by 33.9% (from 6.2 ha to 4.1 ha).

Exposures of the social and ecological elements are assessed considering the intersection between the flood hazard affected area and the land use classes in Norwegian DC. Exposure score maps for both ecosystems and social systems show that ecological and social exposures under both scenarios (with and without NBS) are heterogeneous all over the study area. We estimated ecosystem exposure based on one indicator – proportion of grassland/pasture/forest/water bodies in flooding hazard prone area (EE4) and social exposure based on two indicators – proportion of buildings/properties and proportion of roads. Proportion of population exposed in hazard prone areas was not considered since no residential buildings are exposed to flood hazard in both scenarios. As the NBS implementation is expected to reduce extent and maximum flow depth, it will eventually reduce social and ecological exposure in the flood affected areas. Both ecosystem and social exposure are effectively decreased, specifically in the most threatened area between the two main roads. Similar results are found with the combined score for SES exposure (Fig. 14). This is due to the adoption of the same spatially explicit approach in GIS environment for the calculation of the indicators used to assess both ecosystem and social exposure at Norwegian DC.

4.4.3. Risk assessment in PHUSICOS Norwegian DC – Øyer

SES risk scores for Norwegian DC at the baseline scenario shows that, apart from the Søre Brynsåa riverbed, the areas where flood risk is higher (risk score - Medium Low to Medium, 0.002–0.24) are placed where the two main roads are inundated and in between them (Fig. 15). This is mainly due to high SES exposure and vulnerability scores for these areas. NBS implementation will potentially achieve an overall risk reduction of 35.7%. In detail, NBS implementation lowers medium, medium low and low risk areas of 92%, 29% and 45%, respectively. Moreover, when the NBS is implemented, the road exposed area and the forest and rural exposed area are reduced by 99% and 39%, respectively (Fig. 14).

4.5. Vulnerability and risk assessment in the context of NBS for rockfall: PHUSICOS case study in France

4.5.1. SES vulnerability to rockfall in PHUSICOS French DC – Artouste

As performed in Øyer DC, SES vulnerability to rockfall for French DC is calculated just for current baseline scenario, since NBS implementation is expected to not significantly affect it. The assessment of SES vulnerability to rockfall in French DC reveals that the most vulnerable areas are the RD-934 regional road, the dam on the lake below the road itself and few rural buildings placed along

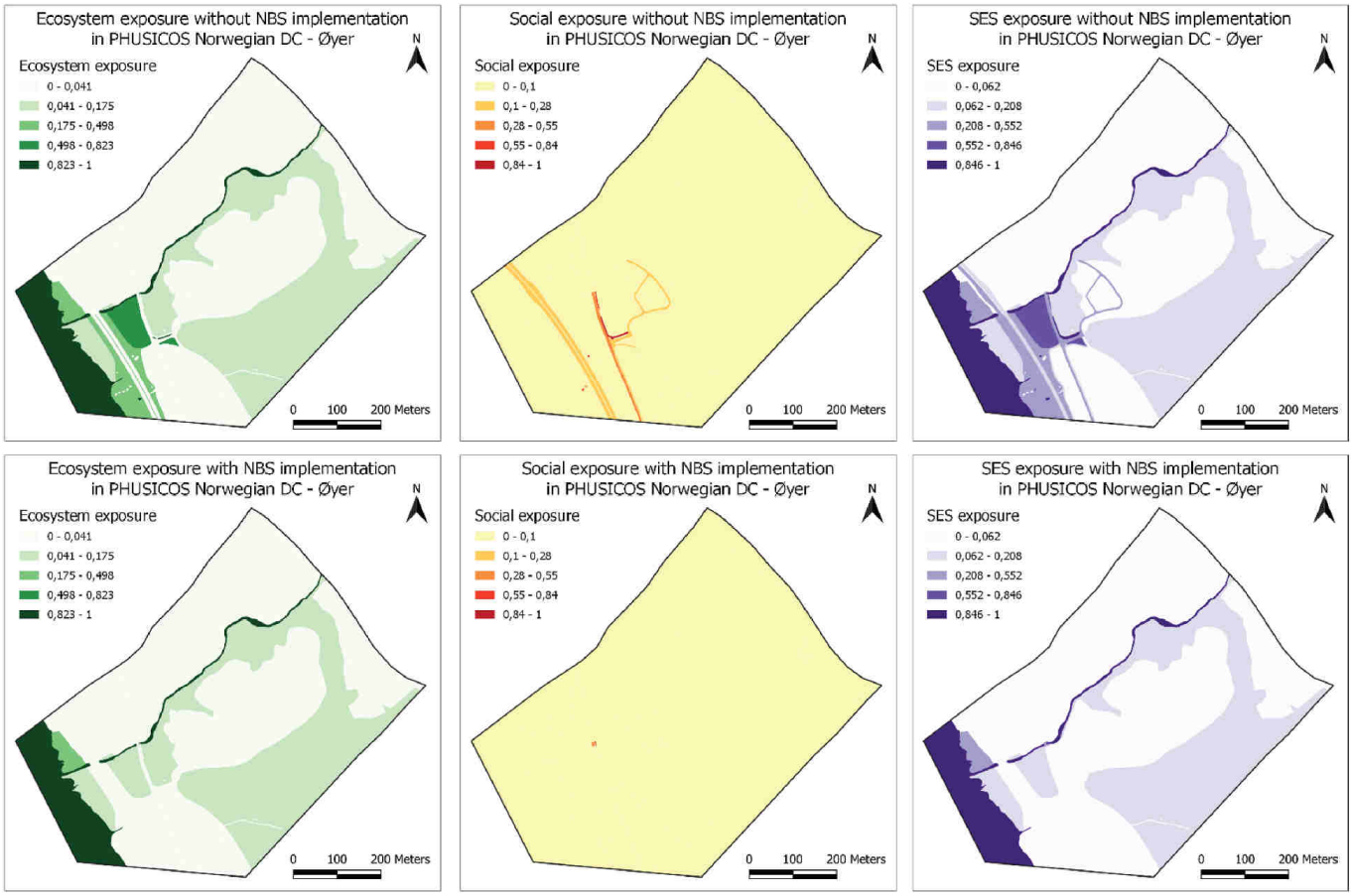

Fig. 14. Ecosystem exposures, social exposures, and the SES exposures (from left to right) in PHUSICOS Norwegian DC under with and without NBS scenarios (bottom and top panels, respectively).

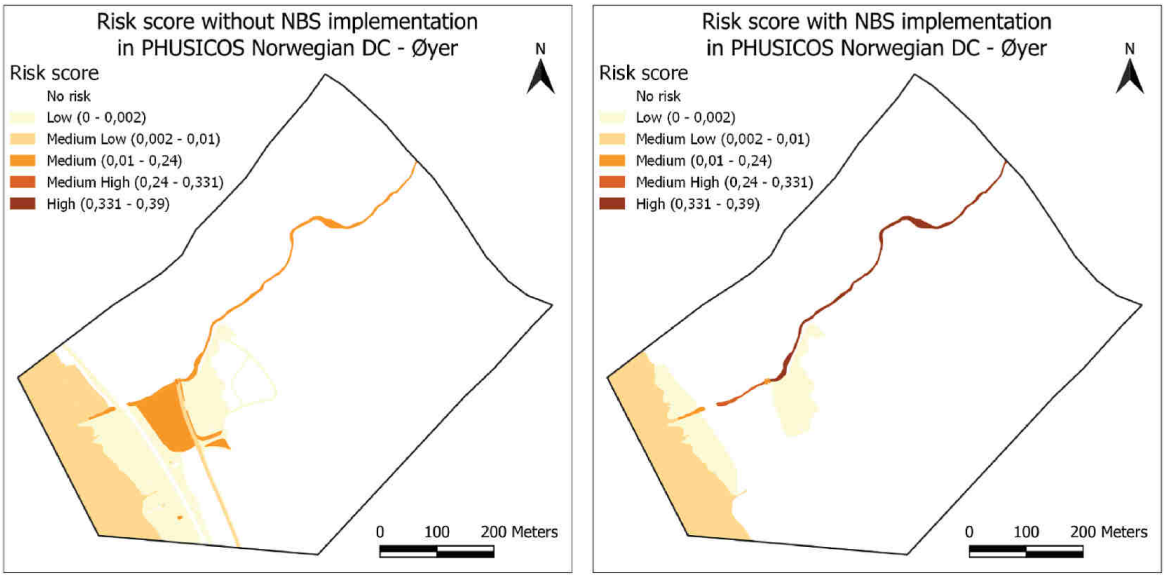

Fig. 15. SES risk scores for a 200-year flood event in PHUSICOS Norwegian DC under without (left) and with (right) NBS scenarios.

the road (Fig. 16). This is mainly due to the high SES lack of ecosystem robustness and capacity due to low mean species abundance (ER2) and considerable landscape fragmentation (ER3).

4.5.2. Hazard and exposure without and with NBS implementation scenarios in PHUSICOS French DC – Artouste

Rockfall hazard is quantified as the product of standardized rockfall maximum kinetic energy and reach probability, expected at each cell of the study area grid ($0.50\ m \times 0.50\ m$), for both the baseline and NBS scenario configurations (i.e., without and with NBS) in case of occurrence of a rockfall from the rocky slope of blocks with 1 m^3 volume, related to a 100-year return period.

The NBS, currently under implementation on the rocky slope above the road in the frame of PHUSICOS project (i.e., wooden tripods, meshes and barriers), is expected to fix and stabilize rock boulders with masses larger than 1500 kg and to stop them as soon as they collapse. Therefore, the two adopted configurations are: i) current situation (without NBS), which is expected to be characterized by high kinetic energies along the slope, and large number of blocks deposited along the slope and, to a lesser extent, on the road; ii) NBS in place, which should ensure an overall reduction of both the maximum kinetic energy and the reach probability all over the area.

Rockfall simulations carried out at French DC [34] for a 100-year return period event in current conditions revealed that the highest rockfall intensities occur in a few small areas, scattered along the slope, and at the base of the south-eastern slope area, although far from the road. A smaller intensity is recorded in the northern part on slopes to the foothill of the highest rocky walls and it locally affects the road close to the main road bend. When the NBS is implemented, despite the overall hazard prone area only slightly decreases, the high intensity areas are expected to be less prevalent than those of baseline scenario. Medium intensity values are recorded in a few areas with a moderately large extension, in the middle of the slope to the foothill of the tallest rock faces. While in the baseline scenario the road and all the forest slope above it are classified as high hazard, after NBS implementation the hazard value of these two land uses decreases, and the forest achieve a reduction of the hazard score (Fig. 17).

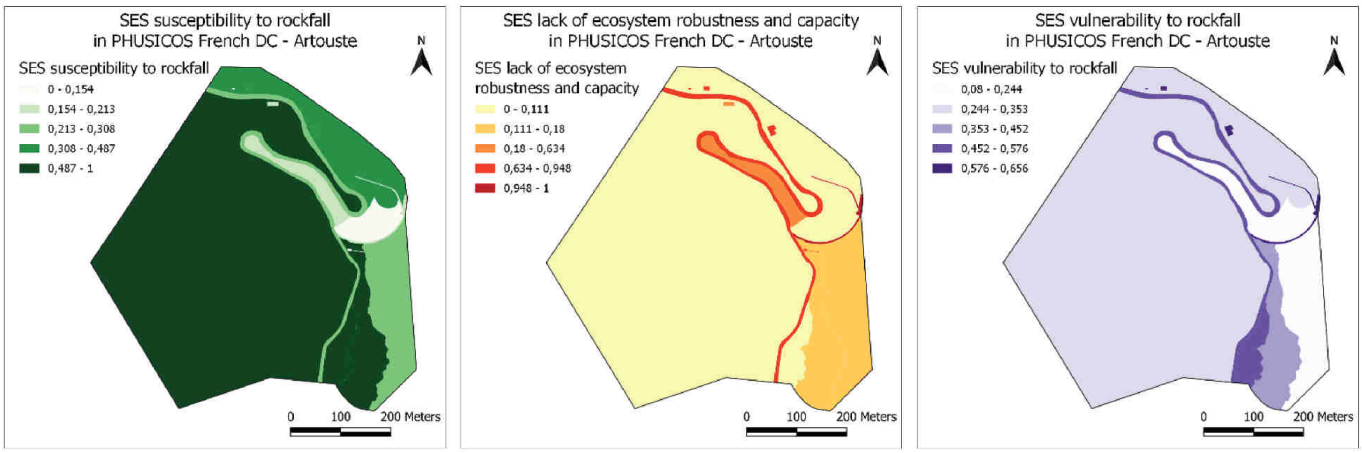

Fig. 16. Social-ecological System (SES) susceptibility (left), lack of ecosystem robustness and capacity (central panel) and final SES vulnerability (right) with respect to floods in PHUSICOS French DC.

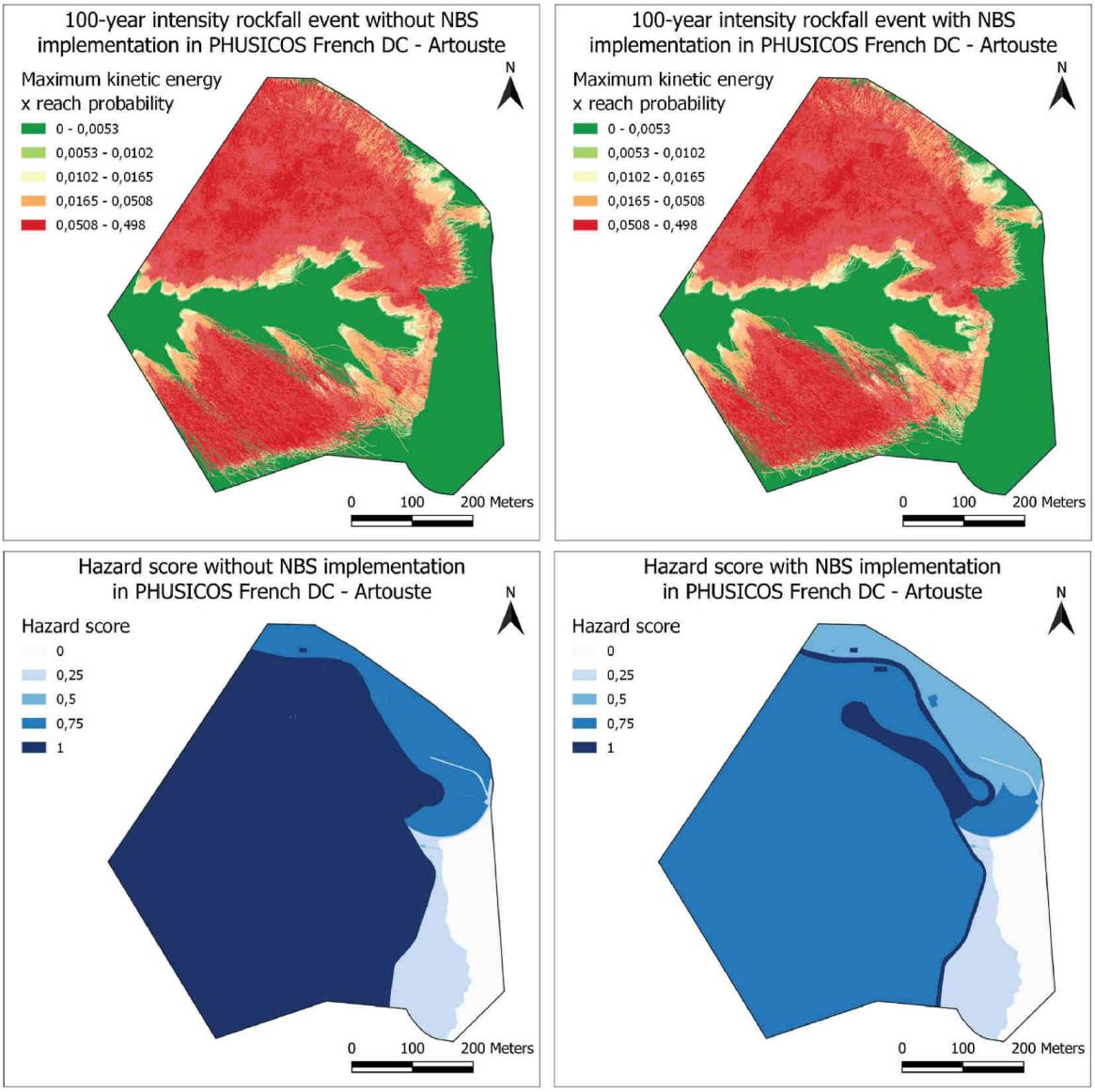

Fig. 17. Extent and hazard scores of rockfall for a 100-year event in the French DC in current conditions (without NBS, left panels) and with wooden tripods, meshes and barriers in place (with NBS, right panels) configurations.

Exposure of the social and ecological components results from the intersection between the rockfall hazard affected area and the land use classes in French DC. It is worth noting that, since there are almost no variations in the overall hazard prone areas extension between baseline and NBS scenario, both ecological and social exposures display the same values. Therefore, social-ecological system exposure score maps for baseline and NBS scenarios are identical. Ecosystem exposure was assessed based on one indicator – proportion of grassland/pasture/forest/water bodies in rockfall hazard prone area (EE5) and social exposure based on two indicators – proportion of buildings/properties and proportion of roads. As occurred in Norwegian DC, proportion of population exposed in hazard prone areas was not considered since the few buildings in the study area are uninhabited. RD-934 regional road, the dam and the few rural buildings along the roads proved to be the most vulnerable land use classes, due to a relevant social exposure value, while the forest covering the rocky slope shows a medium high exposure value given by a high ecosystem exposure (Fig. 18).

4.5.3. Risk assessment in PHUSICOS French DC – Artouste

For French DC, SES Risk assessment revealed how risk scores, for both baseline and NBS scenario, are significantly affected by hazard scores. This is due to the almost null variability in SES exposure values among the two scenarios. Actually, in the baseline scenario, the most at-risk land use classes are the road and the buildings along it, followed by the forest slope above the road itself. NBS implementation could potentially achieve an overall lowering of risk scores and, in detail, a reduction of High-risk areas of 97%. Moreover, when the NBS is implemented, the forest above the road passes from High and Medium-High risk classes to Medium-High and Medium risk classes (Fig. 19).

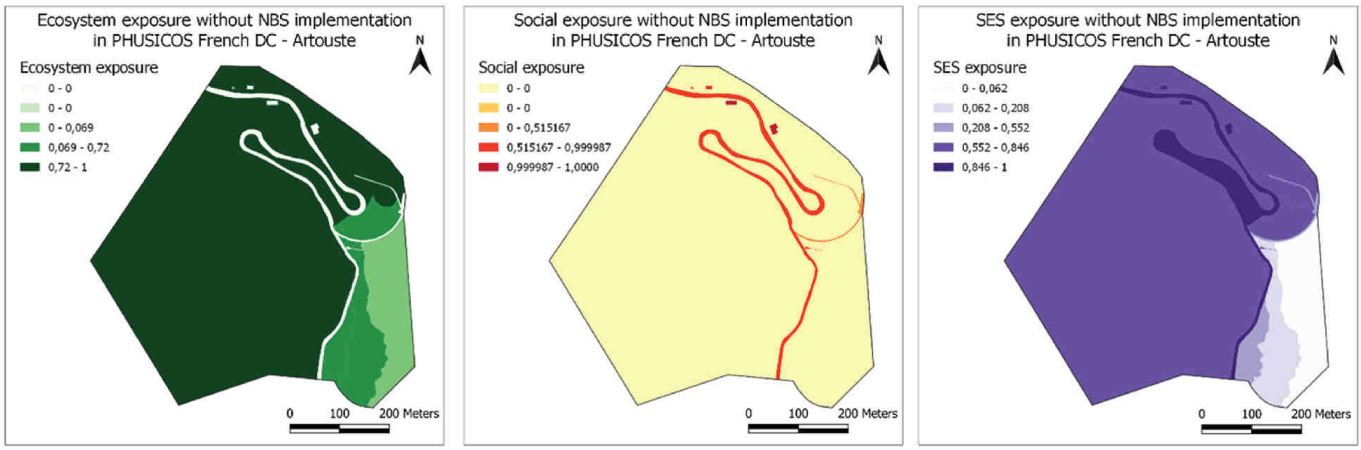

Fig. 18. Ecosystem exposures, social exposures, and the SES exposures (from left to right) in PHUSICOS French DC under without NBS scenario (baseline). The figures for the exposure under NBS scenario are the same.

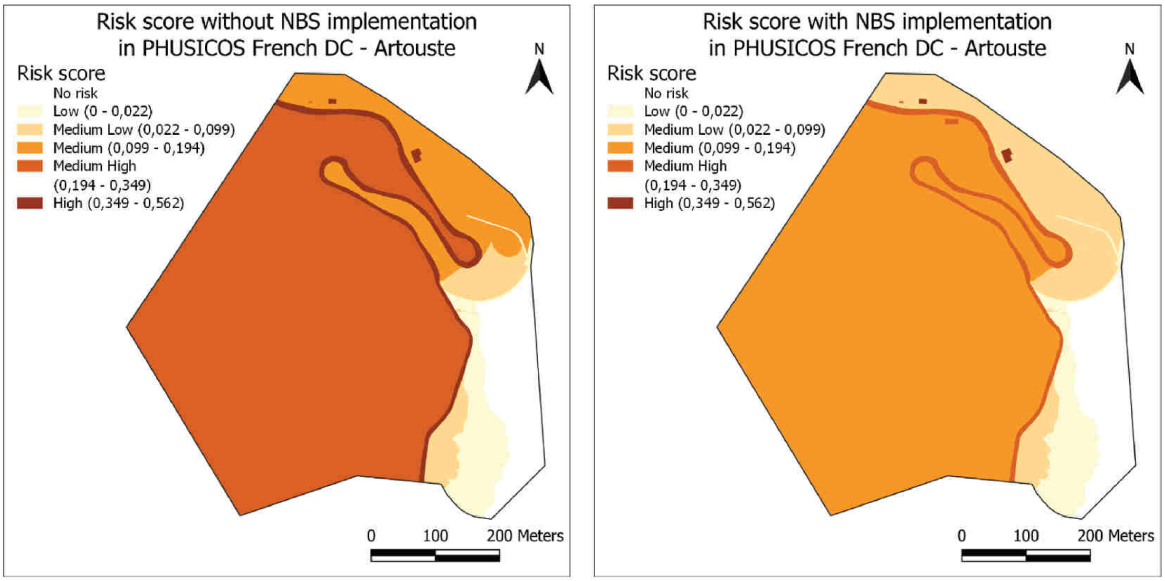

Fig. 19. SES risk scores for a 100-year rockfall event in PHUSICOS French DC under without (left) and with (right) NBS scenarios.

5. Discussion and conclusion

Nature-based solutions implemented in the OALs and DCs have the potential to reduce effectively the risks faced by social-ecological systems. For example, in OAL Italy Panaro and OAL UK, the surface areas of the landscapes that fall under the higher risk scores are reduced when NBS are implemented. The results are based on modelling simulations of hazards with and without NBS scenarios and the use of an indicator-based risk assessment framework that captures all the dimensions of risk both for the social and ecological components of the system (VR-NBS framework). This was the first time the VR-NBS framework was implemented and through the selected five case study areas in Europe, our results show that the framework allows capturing the potential effects of NBS in reducing risks related to HMH. Overall, the approach clearly showed that the framework provides users with the opportunity to understand the effects an NBS can have on the various components of risks. The indicator library affords the user the flexibility to conduct specific analysis for a given setting, moving away from fixed and rigid indicator frameworks. The case studies were highly diverse in terms of hazards they experience, their SES, and their scale. There are however limitations to the approach and additional assessments and further research are required to test the framework further and capture additional dimensions of NBS risk reduction functions. This is discussed further below.

The first limitation was linked to data availability as is often the case with these types of assessment (e.g., Ref. [7]. The research had to draw on secondary data (population census and other national and global statistics) and remote sensing-based data. Primary data, as originally envisaged, could not be collected due to travel restrictions during the COVID-19 pandemic. Secondary data were drawn from different sources and for different years, implying that in some cases, they could not reflect the current situation accurately. For some indicators, global databases (e.g., Global Biodiversity Index) were used to represent the situation at the local level. In some cases (e.g., OAL UK and OAL Austria, as well as PHUSICOS DCs), regional data such as population density and employment rate had to be used. True representation at the local level was therefore not achieved. We have also used some proxy indicators such as Biodiversity Intactness Index and Baseline Water Stress as alternatives due to the lack of data for some of the originally selected indi-

cators. The use of proxy indicators is, however, a common practice in these types of assessments [7,8]. One approach to address these limitations is to collect data through, for example, household surveys or online questionnaires. This is, however, time consuming and would need to be repeated on a regular basis to update the assessment, which would not be possible through classical project funding cycles. Increasingly, the use of remotely sensed data and information can be considered to quantify some indicators, but this will not cover all the dimensions of risk and in particular some of the social characteristics of the system.

Second, in the context of OAL Italy Panaro and the French DC, we considered only maximum potential flood and rockfall reduction scenarios with the implementation of NBS at full scale, respectively. In practical conditions, there will be a time lag between the implementation of NBS and effective performance for risk reduction [11,41], as the NBS will mature over time and provide gradual hazard reduction functions. This implies that time series of indicators are required to capture the NBS maturity time lag, which was not readily available through the OPERANDUM and PHUSICOS projects. This type of scenario analysis also shows the potential application of the risk assessment approach for monitoring the performance of NBS for risk reduction over time. The study used a number of socio-economic and ecological indicators which change over time and can affect vulnerability, exposure and risk. Furthermore, an indicator representing vegetation conditions (i.e., NDVI) was used, which is directly linked to the plant-based NBS (e.g., grass cover for embankment strengthening in OAL Italy, plantation for reducing landslide in the UK, Austria and France). The maturation of NBS could be monitored over the years as the plants grow and the reduction of risk could be assessed periodically by using the VR-NBS framework. Regular monitoring of the indicators and assessment of vulnerability and risk of SES could better inform the decision makers on how the NBS is providing benefits or negative impacts [42]. Understanding both seasonal and annual variability through indicators would be important, as the performance of NBS could be affected by such temporal variability [43].

Third, in all our case studies, we mainly demonstrated the effects of the NBS on the hazard and, deriving from that, the exposure components of risk. This was possible thanks to the extensive modelling activities conducted in both OPERANDUM and PHUSICOS projects. However, we could not project the vulnerability of SES for the same time frame as the impact modelling was done. We therefore could not demonstrate the effects of the NBS on reducing vulnerability, but again, the framework allows to capture this dimension. In some cases, the effects of an NBS beyond the hazard component might be difficult to quantify. This is, for example, when the NBS occupies a relatively small portion of a larger landscape. This can be illustrated with the OAL Italy Panaro case study where the NBS consists of herbaceous vegetation planted on the embankment of the Panaro River. The co-benefits of the NBS beyond the immediate consolidation of the embankments are minimal in the context of the large geographical area concerned by the risk reduction measure. The risk assessment results could be further improved if the projected values for vulnerability and in some cases, exposure indicators are obtained. It is often difficult and requires additional time and resources for generating projected scenarios of socio-economic and ecological conditions because of data unavailability and methodological limitations [7]. Despite limitations in calculating vulnerability and exposure under 'with NBS scenario' in the OPERANDUM OALs and the PHUSICOS DCs, the risk assessment results show the potential application of the VR-NBS framework in the context of NBS projects in all the OALs and DCs.

Fourth, the small spatial scale of the OALs and DCs restricts the use of the framework through the need to acquire data at the very local scale (discussed above) and by making it more difficult to create vulnerability and risk maps that show spatial variation. One exception was OAL Italy Panaro where municipalities were taken as the spatial unit of analysis, and for which data for many socio-economic indicators were available from well-documented and easily available census statistics. However, the data available for socio-economic indicators were limited in the other four, smaller case studies which were typically located within one municipality or census region. Census-based data for socio-economic indicators have only one value for each municipality or census block which gives a single value for the entire OAL or DC in these four case studies. Municipality or census block-based census data or other secondary data can be suitable for vulnerability and risk assessment at a larger scale (regional or country level) [7,8], but primary data will give more meaningful results at the exact scale of application. Furthermore, to visualize the differences in vulnerability and risk within the smaller OALs (the UK and Austria) and the two DCs, we have used land use boundaries. This allowed us to assign values for SES vulnerability and exposure indicators to specific land use categories. However, there might be local variation within the land use boundaries. For example, the area with forest land use may have differences in land slope and soil characteristics that may influence the vulnerability of SES to potential landslide hazard [44]. A suitable alternative to better capture local variation is to use moderate spatial resolution raster data (e.g., 30 *m*–100 *m* pixel size), which can show variations within the same land use areas [45]. We have used some ecological indicators, such as NDVI (30 *m* resolution), Global Biodiversity Intactness Index (1 km resolution), which enabled capturing spatial variation of ecological vulnerability. Hazard mapping was independent of land use boundaries, rather it was based on potential hazard zones determined by the observed historical record of hazard prone areas within the OALs and DCs. An average hazard score was given to each land use boundary or municipality while calculating risk. Scale issues are also relevant to characterizing the hazard. For example, in the case of OAL Italy Panaro, the study considered the effect of the NBS only at one location, while a more comprehensive analysis should consider all potential failure/overtopping locations along the river.

The limitations above are not specific to the VR-NBS framework but through this first implementation of the framework, we were able to demonstrate the advantages and shortcomings of its application. The framework allows to capture the effects NBS can have on risk reduction from HMH. The use of a flexible indicator library allows to carry out risk assessments that are specific to a given SES-hazard combination. One has, however, to be careful not to select indicators simply because they are likely to show an effect of the NBS in terms of risk reduction. As for any risk assessment, the relevance of each indicator used needs to be justified for the risk dimension it is being considered for (social susceptibility, ecosystem robustness, etc.). The framework and the approach in general are better suited for landscapes that have high heterogeneity in their underlying characteristics both in the social and ecological domains. In these cases, spatial differentiation of risks and of the effect of the NBS in reducing these risks can be explicitly quantified and visualised.

While the study has focused on the effect of NBS on reducing hydro-meteorological risk, further research could be carried out to compare the effectiveness of NBS and grey infrastructures to reduce the same risk, which will help policymakers to take better decisions. The framework could in the future be applied with more indicators quantified through existing data or through the collection of specific data and information. The approach gives a robust estimation of relative risk reduction potential and can be refined by combining it with additional tools including cost-benefit analyses. As a next step, it will be important to discuss the framework and its application further with decision-makers in order to determine the additional value it may bring to tools and approaches agencies dealing with risk assessment and risk reduction measures already use.

Funding

This work was supported by the European Union's Horizon 2020 research and innovation programme. It was funded by and carried out within the framework of OPERANDUM (OPEn-air laboRAtories for Nature baseD solUtions to Manage hydro-meteo risks) project (Grant no. 776848) and PHUSICOS project (Grant no. 776681).

Declaration of competing interest

The authors declare that they have no known competing financial interests or personal relationships that could have appeared to influence the work reported in this paper.

Data availability

Data will be made available on request.

Acknowledgement

Authors involved in PHUSICOS project are sincerely grateful to Anders Solheim (Norwegian Geotechnical Institute), Mari Olsen and Trine Frisli Fjøsne (Innlandet County Authority), Didier Vergés (Consorcio de la Communauté de Travail des Pyrénées), Séverine Bernardie (BRGM), Santiago Fàbregas Reigosa (AECT Pirineos-Pyrénées), José Carlos Robredo Sánchez (Universidad Politécnica de Madrid) for providing us with some input data for modelling.

Appendix A. Supplementary data

Supplementary data to this article can be found online at https://doi.org/10.1016/j.ijdrr.2023.103771.

References

[1] CEED and UNDRR, *Human Cost Of Disasters: an Overview Of the Last 20 Years, 2000-2019*. UN Office for Disaster Risk Reduction, 2020.
[2] IPCC, in: H.-O. Pörtner, D.C. Roberts, M. Tignor, E.S. Poloczanska, K. Mintenbeck, A. Alegría, M. Craig, S. Langsdorf, S. Löschke, V. Möller, A. Okem, B. Rama (Eds.), *Climate Change 2022: Impacts, Adaptation, and Vulnerability*. Contribution of Working Group II to the Sixth Assessment Report of the Intergovernmental Panel on Climate Change, Cambridge University Press. Cambridge University Press, Cambridge, UK and New York, NY, USA, 2022, p. 3056, https://doi.org/10.1017/9781009325844.
[3] UNISDR, Sendai Framework for Disaster Risk Reduction 2015–2030, United Nations Office for Disaster Risk Reduction (UNISDR), Geneva, Switzerland, 2015.
[4] United Nations, *Nature-based Solutions for Supporting Sustainable Development*, Resolution 5 of United Nations Environment Assembly Adopted on 2 March 2022, 2022 Retrieved on June 05, 2022, from. https://wedocs.unep.org/bitstream/handle/20.500.11822/39864/NATURE-BASED%20SOLUTIONS%20FOR%20SUPPORTING%20SUSTAINABLE%20DEVELOPMENT.%20English.pdf?sequence=1&isAllowed=y.
[5] E. Cohen-Shacham, G. Walters, C. Janzen, S. Maginnis (Eds.), Nature-based Solutions to Address Global Societal Challenges, IUCN, Gland, Switzerland, 2016 xiii + 97pp.
[6] M. Damm, Mapping Social-Ecological Vulnerability to Flooding, University of Bonn, Germany, 2010 PhD thesis. https://core.ac.uk/download/pdf/304638754.pdf.
[7] M. Hagenlocher, F.G. Renaud, S. Haas, Z. Sebesvari, Vulnerability and risk of deltaic social-ecological systems exposed to multiple hazards, Sci. Total Environ. 631 (2018) 71–80.
[8] C.C. Anderson, F.G. Renaud, M. Hagenlocher, J.W. Day, Assessing multi-hazard vulnerability and dynamic coastal flood risk in the Mississippi Delta: the Global Delta Risk Index as a social-ecological systems approach, Water 13 (4) (2021) 577.
[9] Z. Sebesvari, F.G. Renaud, S. Haas, Z. Tessler, M. Hagenlocher, J. Kloos, C. Kuenzer, A review of vulnerability indicators for deltaic social–ecological systems, Sustain. Sci. 11 (4) (2016) 575–590, https://doi.org/10.1007/s11625-016-0366-4.
[10] M. Hagenlocher, I. Meza, C. Anderson, A. Min, F.G. Renaud, Y. Walz, S. Siebert, Z. Sebesvari, Drought vulnerability and risk assessments: state of the art, persistent gaps, and research agenda, Environ. Res. Lett. 14 (8) (2019) 083002, https://doi.org/10.1088/1748-9326/ab225d.
[11] M.A.R. Shah, F.G. Renaud, C.C. Anderson, A. Wild, A. Domeneghetti, A. Polderman, W. Zixuan, A review of hydro-meteorological hazard, vulnerability, and risk assessment frameworks and indicators in the context of nature-based solutions, Int. J. Disaster Risk Reduc. 50 (2020) 101728, https://doi.org/10.1016/j.ijdrr.2020.101728.
[12] Y. Peng, N. Welden, F.G. Renaud, A framework for integrating ecosystem services indicators into vulnerability and risk assessments of deltaic social-ecological systems, J. Environ. Manag. 326 (2022) 116682.
[13] A. Alves, B. Gersonius, Z. Kapelan, Z. Vojinovic, A. Sanchez, Assessing the Co-Benefits of green-blue-grey infrastructure for sustainable urban flood risk management, J. Environ. Manag. 239 (2019) 244–254.
[14] W. Chen, W. Wang, G. Huang, Z. Wang, C. Lai, Z. Yang, The capacity of grey infrastructure in urban flood management: a comprehensive analysis of grey infrastructure and the green-grey approach, Int. J. Disaster Risk Reduc. 54 (2021) 102045.
[15] F. Pugliese, G. Caroppi, A. Zingraff-Hamed, G. Lupp, C. Gerundo, Assessment of NBSs effectiveness for flood risk management: the Isar River case study, J. Water Supply Res. Technol. - Aqua 71 (1) (2022) 42–61, https://doi.org/10.2166/aqua.2021.101.
[16] G. Caroppi, F. Pugliese, C. Gerundo, F. De Paola, M. Stanganelli, G. Urciuoli, M. Giugni, A comprehensive framework tool for performance assessment of NBS for hydro-meteorological risk management, J. Environ. Plann. Manag. (2023), https://doi.org/10.1080/09640568.2023.2166818.
[17] European Commission, Evaluating the Impact of Nature-Based Solutions: a Handbook for Practitioners, Publications Office of the European Union, Directorate-General for Research and Innovation, 2021. https://data.europa.eu/doi/10.2777/244577.
[18] IPCC, Managing the risks of extreme events and disasters to advance climate change adaptation, in: C.B.V. Field, T.F. Barros, D.Q. Stocker, K.L. DJ Dokken,

M.D. Ebi, K.J. Mastrandrea, G.K. Mach, S.K. Plattner, M. Allen, & P.M. Tignor, Midgley (Eds.), A Special Report of Working Groups I and II of the Intergovernmental Panel on Climate Change, Cambridge University Press, Cambridge, UK, and New York, 2012.
[19] C. Moos, P. Bebi, M. Schwarz, M. Stoffel, K. Sudmeier-Rieux, L. Dorren, Ecosystem-based disaster risk reduction in mountains, Earth Sci. Rev. 177 (2018) 497–513.
[20] S.M. Alfieri, F. Foughnia, R. Lindenbergh, M. Menenti, Extent of Severe Flooding Events in the Panaro River, Italy (OAL-IT), 2021 https://doi.org/10.5281/zenodo.5336400 (Version V01) [Data set]. Zenodo.
[21] European Environment Agency, Copernicus Land Monitoring Service 2018, 2018.
[22] J. Pfeiffer, T. Zieher, J. Schmieder, M. Rutzinger, U. Strasser, Spatio-temporal assessment of the hydrological drivers of an active deep-seated gravitational slope deformation: the Vögelsberg landslide in Tyrol (Austria), Earth Surf. Process. Landforms 46 (10) (2021) 1865–1881, https://doi.org/10.1002/esp.5129.
[23] J. Pfeiffer, T. Zieher, J. Schmieder, T. Bogaard, M. Rutzinger, C. Spötl, Spatial assessment of probable recharge areas–investigating the hydrogeological controls of an active deep-seated gravitational slope deformation, Nat. Hazards Earth Syst. Sci. 22 (7) (2022) 2219–2237 https://doi.org/10.5194/nhess-22-2219-2022, 2022.
[24] J. Pfeiffer, T. Zieher, B. Schneider-Muntau, Slope stability evolution of a deep-seated landslide considering a constantly deforming topography, Earth Surf. Process. Landforms (2023) 1–17, https://doi.org/10.1002/esp.5527.
[25] A. Gonzalez-Ollauri, S.B. Mickovski, Plant-Best: a novel plant selection tool for slope protection, Ecol. Eng. 106 (2017) 154–173, https://doi.org/10.1016/j.ecoleng.2017.04.066.
[26] A. Gonzalez-Ollauri, S.B. Mickovski, Shallow landslides as drivers for slope ecosystem evolution and biophysical diversity, Landslides 14 (5) (2017) 1699–1714, https://doi.org/10.1007/s10346-017-0822-y.
[27] D.P. Roy, M.A. Wulder, T.R. Loveland, C.E. Woodcock, R.G. Allen, M.C. Anderson, Z. Zhu, Landsat-8: science and product vision for terrestrial global change research, Rem. Sens. Environ. 145 (2014) 154–172.
[28] T. Newbold, L.N. Hudson, A.P. Arnell, S. Contu, A. De Palma, S. Ferrier, A. Purvis, Has land use pushed terrestrial biodiversity beyond the planetary boundary? A global assessment, Science 353 (6296) (2016) 288–291.
[29] A.M. Schipper, J.P. Hilbers, J.R. Meijer, L.H. Antão, A. Benítez-López, M.M. de Jonge, M.A. Huijbregts, Projecting terrestrial biodiversity intactness with GLOBIO 4, Global Change Biol. 26 (2) (2020) 760–771.
[30] K. McGarigal, FRAGSTATS: Spatial Pattern Analysis Program for Quantifying Landscape Structure, 351, US Department of Agriculture, Forest Service, Pacific Northwest Research Station, 1995.
[31] M. Drusch, U. Del Bello, S. Carlier, O. Colin, V. Fernandez, F. Gascon, P. Bargellini, Sentinel-2: ESA's optical high-resolution mission for GMES operational services, Rem. Sens. Environ. 120 (2012) 25–36.
[32] Joint Research Centre-European Commission, Handbook on Constructing Composite Indicators: Methodology and User Guide, OECD publishing, 2008.
[33] C. Spyrou, E. Apostolidou, A. Mentzafou, L. Jia, *Multi-impacts Assessment for OAL and NBS - Part A,* Deliverable 5.2, OPEn-Air laboRAtories for Nature baseD solUtions to Manage Hydro-Meteo Risks (OPERANDUM), Italy, 2020. https://www.operandum-project.eu/wp-content/uploads/D5.2a-Multi-impacts-assessment-for-OAL-and-NBS.pdf.
[34] A. Pignalosa, C. Gerundo, F. Pugliese, G. Speranza, P. Budetta, A. Corniello, M. Stanganelli, F. De Paola, Deliverable D4.4 (project deliverable PHUSICOS). https://phusicos.eu/wp-content/uploads/2019/01/220322_D4.4_Task4.4_final_compressed.pdf, 2022.
[35] N. Lu, J.W. Godt, Hillslope Hydrology and Stability, Cambridge University Press, New York, USA, 2013.
[36] T. Zieher, M. Bremer, M. Rutzinger, J. Pfeiffer, P. Fritzmann, V. Wichmann, Assessment of landslide-induced displacement and deformation of above-ground objects using UAV-borne and airborne laser scanning data, ISPRS Annals of Photogrammetry, Remote Sensing & Spatial Information Sciences (2019) 461–467 https://doi.org/10.5194/isprs-annals-IV-2-W5-461-2019, IV-2/W5.
[37] J. O'Brien, R. Garcia, FLO-2D Reference Manual, Version 2009. Available online: 2009 docs.dicatechpoliba.it/filemanager/303/PROTEZIONE%20IDRAULICA%202016-2017/3.3_FLO-2D%20Reference%20Manual %202009.pdf. (Accessed 7 October 2021).
[38] A. Gonzalez-Ollauri, S.B. Mickovski, A simple GIS-based tool for the detection of landslide-prone zones on a coastal slope in Scotland, Land 10 (7) (2021) 685.
[39] C. Gerundo, G. Speranza, A. Pignalosa, F. Pugliese, F. De Paola, A methodological approach to assess nature-based solutions' effectiveness in flood hazard reduction: the case study of gudbrandsdalen valley, Environmental Science Proceedings 21 (1) (2022) 29, https://doi.org/10.3390/environsciproc2022021029.
[40] Norwegian Mapping Authority, National Website for Map Data and Other Location Information in Norway. Kartverket, 2021 Available online: http:///www.geonorge.no. (Accessed 1 October 2021).
[41] S. Han, C. Kuhlicke, Barriers and drivers for mainstreaming nature-based solutions for flood risks: the case of South Korea, International Journal of Disaster Risk Science 12 (5) (2021) 661–672.
[42] C. Albert, M. Brillinger, P. Guerrero, S. Gottwald, J. Henze, S. Schmidt, B. Schröter, Planning nature-based solutions: principles, steps, and insights, Ambio 50 (8) (2021) 1446–1461.
[43] P. Kumar, S.E. Debele, J. Sahani, N. Rawat, B. Marti-Cardona, S.M. Alfieri, T. Zieher, An overview of monitoring methods for assessing the performance of nature-based solutions against natural hazards, Earth Sci. Rev. 217 (2021) 103603.
[44] T. de Jesús Arce-Mojica, U. Nehren, K. Sudmeier-Rieux, P.J. Miranda, D. Anhuf, Nature-based solutions (NbS) for reducing the risk of shallow landslides: where do we stand? Int. J. Disaster Risk Reduc. 41 (2019) 101293.
[45] A.M. Dewan, Y. Yamaguchi, Land use and land cover change in Greater Dhaka, Bangladesh: using remote sensing to promote sustainable urbanization, Appl. Geogr. 29 (3) (2009) 390–401.